Università degli Studi di Padova

Dipartimento di Biologia

SCUOLA DI DOTTORATO DI RICERCA IN BIOSCIENZE E BIOTECNOLOGIE

INDIRIZZO NEUROBIOLOGIA

CICLO XXVIII

Molecular identification of ATP sensitive Mitochondrial Potassium Channel (mitoK$_{ATP}$)

Direttore della Scuola : Ch.mo Prof. Paolo Bernardi

Coordinatore d'indirizzo: Ch.ma Prof. Daniela Pietrobon

Supervisore: Ch.mo Prof. Rosario Rizzuto

Co-Supervisor: Dott. Diego De Stefani

Dottorando: Angela Paggio

TABLE OF CONTENTS

SUMMARY

Mitochondria ATP-sensitive potassium channels (mitoK$_{ATP}$) were first described in 1991 by direct patch clamp of isolated mitoplasts (i.e. mitochondria lacking the outer membrane). Since then, a growing amount of evidences showed that they are implicated in the control of a variety of mitochondrial functions. Most importantly, pharmacological modulation of the mitoK$_{ATP}$ can efficiently protect the heart from ischemia/reperfusion injury. However, despite its huge therapeutic potential, the molecular identity of the mitoK$_{ATP}$ is still unknown. Here we identify a protein complex that is sufficient to reconstitute a functional K^+ permeant channel with the same pharmacological profile of the mitoK$_{ATP}$. In particular, we demonstrate that the mitoK$_{ATP}$ is a heterooligomer composed by two different components. One is a previously uncharacterized protein of unknown function that we now name "mitoK" (formerly known as coiled-coil domain containing protein 51, CCDC51). The other is a protein belonging to the ABC superfamily (formerly known as ABCB8) here named "mitoSUR". It possesses a nucleotide-binding site (a standard Walker motif) and provides ATP sensitivity to the mitoK pore-forming subunit through direct protein interaction.

In detail, we demonstrated that mitoK is a mitochondrial protein located in the inner mitochondrial membrane (IMM), with two transmembrane domains and both its N- and C-termini exposed to the organelle matrix. Its overexpression induces a decrease in mitochondrial Ca^{2+} transients evoked by agonist stimulation, a drastic reduction of mitochondria membrane potential, fragmentation of the mitochondrial network and a derangement of the IMM ultrastructure, with the total collapse of the cristae. However, all these effect can be rescued by the concomitant overexpression of mitoSUR, but not by the expression of the mitoSUR^{K513A} mutant that lacks ATP binding. Most importantly, in vitro reconstitution of purified mitoK and mitoSUR in a planar lipid bilayer form a channel i) selective for monovalent cations, ii) blocked by tetraethyl ammonium (TEA, a general inhibitor of K^+ channels), iii) sensitive to ATP, iv) activated by diazoxide and v) inhibited by 5-HD.

Finally, we focused our efforts to understand the physiological role of mitoK$_{ATP}$. According to the available literature, mitoK$_{ATP}$ channels are believed to be protective in

ischemia/reperfusion injury. However, the broad conservation profile among all vertebrates suggests that the mitoK$_{ATP}$ should also have a primary housekeeping function. In order to analyze the genuine physiological role of the mitoK$_{ATP}$, we generated Hela cells knockout for mitoK by using the Crispr/Cas9 technology. Two different guides targeting different gene regions were validated and several Hela mitoK^{KO} clones were obtained. Overall, ablation of mitoK leads to no gross defects in mitochondria morphology, although an impairment of cristae structure becomes evident through electron microscopy. Mitochondrial membrane potential is overall intact and expression of respiratory chain complexes is unaffected. However, we noticed that Hela mitoK^{KO} cells undergo to asynchronous, rapid and transient depolarizations of single mitochondria, a phenome known as “flickering” of mitochondria membrane potential. Therefore, oxygen consumption rate (OCR) is greatly impaired in Hela mitoK^{KO} cells when compared to their wild type counterparts, in both basal, leaky (oligomycin induced) and maximal (i.e. FCCP induced) respiration. As already reported, mitochondrial K^+ homeostasis is fundamental to regulate mitochondrial matrix volume: while excessive accumulation leads to organelle swelling, a decrease in K^+ uptake is predicted to cause matrix contraction, with obvious consequences on the performance of the oxidative phosphorylation. Overall, our data indicates that mitoK$_{ATP}$ is a central regulator of mitochondrial function that modulates the efficiency of energy production according to the ATP availability through the regulation of matrix volume.

RIASSUNTO

I canali mitocondriali del potassio sensibili all'ATP (mitoK$_{ATP}$) sono stati descritti per la prima volta nel 1991 in seguito ad esperimento di patch clamp su mitoplasti (mitocondri privi della membrana mitocondriale esterna) isolati. Da allora, un numero crescente di esperimenti ha dimostrato il coinvolgimento di questi canali nella regolazione di numerose funzioni mitocondriali. In particolare, la modulazione farmacologia di questi canali può efficacemente proteggere il cuore dal danno da ischemia/riperfusione. Tuttavia, nonostante il loro enorme potenziale terapeutico, la struttura molecolare dei canali mitoK$_{ATP}$ è ancora oggi sconosciuta. In questo lavoro abbiamo identificato un complesso proteico permeabile al K^+ con lo stesso profilo farmacologico dei canali mitoK$_{ATP}$. In particolare, abbiamo dimostrato come questi canali siano composti da due differenti subunità. Una di queste è una proteina non ancora caratterizzata dal punto di vista biologico e con funzione sconosciuta, che d'ora in poi chiameremo "mitoK" (precedentemente nota come CCDC51). L'altra componente del canale è una proteina appartenente alla superfamiglia delle proteine ABC (precedentemente nota come ABCB8), che chiameremo "mitoSUR". Quest'ultima possiede un dominio in grado di legare ATP (chiamato "dominio Walker") attraverso cui fornisce sensibilità ai canali mitoK$_{ATP}$ attraverso una interazione diretta con mitoK.

In particolare, abbiamo dimostrato che mitoK è una proteina mitocondriale sita sulla membrana mitocondriale interna, con due domini transmembrana e le rispettive porzioni N- e C- terminale esposte nella matrice. La sovraespressione di mitoK induce una diminuzione dell'accumulo mitocondriale dello ione calcio in risposta a stimoli, una drastica riduzione del potenziale di membrana mitocondriale, frammentazione della morfologia mitocondriale ed una perdita totale delle cristae. Tuttavia, le normali funzioni mitocondriali possono essere recuperate attraverso la contemporanea sovraespressione di mitoSUR, ma non dall'espressione del mutante mitoSUR^{K513A} mancante del dominio che lega ATP. Inoltre, l'espressione in vitro delle proteine purificate mitoK e mitoSUR ed il loro inserimento in una membrana artificiale ci ha permesso di studiarne le caratteristiche elettrofisiologiche, dimostrando che mitoK e mitoSUR formano un canale i) selettivo per cationi monovalenti, ii) inibito da ammonio tetraetile (TEA, un inibitore generico per i canali K^+), iii) sensibile ad ATP, iv) attivato da diazossido e v) inibito da 5-HD.

Infine abbiamo cercato di comprendere il ruolo fisiologico dei canali mitoK$_{ATP}$. Secondo la letteratura disponibile, questi canali hanno un ruolo protettivo nel danno da ischemia/riperfusione. Tuttavia, l'ampio profilo di conservazione tra tutti i vertebrati suggerisce che i canali mitoK$_{ATP}$ abbiano prima di tutto un ruolo nel controllo delle normali funzioni mitocondriali. Al fine di analizzare il vero e proprio ruolo fisiologico di questi canali mitoK$_{ATP}$, abbiamo generato cellule Hela prive del gene che codifica per mitoK utilizzando la tecnologia Crispr/Cas9. Utilizzando due differenti guide in grado di riconoscere due diverse regioni del gene sono stati ottenuti alcuni cloni cellulari privi di mitoK a livello proteico. Nel complesso, la mancanza di mitoK non comporta alcun difetto in termini di morfologia mitocondriale, anche se è evidente una diversa strutture delle cristae attraverso la microscopia elettronica. Il potenziale di membrana mitocondriale è complessivamente intatto e l'espressione dei complessi della catena respiratoria è inalterata. Tuttavia, abbiamo notato che le cellule Hela mitoK^{KO} vanno incontro a depolarizzazioni asincrone, rapide e transitorie, caratteristiche di un fenomeno conosciuto come "flickering" del potenziale di membrana mitocondriale. Abbiamo inoltre osservato che il consumo di ossigeno (OCR) è notevolmente ridotto in questi cloni rispetto alle cellule di controllo, sia in termini di respirazione basale che massimale. Dalla letteratura è infatti noto che l'omeostasi mitocondriale del potassio è fondamentale per regolare il volume della matrice mitocondriale; mentre un accumulo eccesivo di K^+ comporta un aumento del volume, una diminuzione dell'accumulo di K^+ può causare la contrazione della matrice, con ovvie conseguenze sulle prestazioni della fosforilazione ossidativa. Nel complesso, i nostri dati indicano che i canali mitoK$_{ATP}$ regolano le funzioni mitocondriali, modulando l'efficienza della produzione di energia secondo la disponibilità di ATP attraverso la regolazione del volume della matrice.

INTRODUCTION

MITOCHONDRIA

The general framework

Mitochondria are dynamic organelles that are involved in a number of essential cellular processes. They play an important role in energy metabolism as the majority of the cellular ATP is generated via oxidative phosphorylation. In addition, mitochondria are the major source of reactive oxygen species (ROS), which play pivotal roles in signaling and cell injury. In higher eukaryotes mitochondria play a major role in the regulation of apoptosis. Based on these vital processes, many human diseases are linked to mitochondrial dysfunctions, including neurodegenerative diseases (Alzheimer's, Parkinson's, Hungtinton's), motoneuron disorders (amyotrophic lateral sclerosis, type 2A Charcot-Marie-Tooth neuropathy), autosomal dominant optic atrophy, ischemia-reperfusion injury, diabetes, ageing and cancer (Duarte et al., 2014; Gaude and Frezza, 2014). In addition, mutations in mitochondrial DNA cause a variety of pathologies, including MELAS (Mitochondrial Encephalopathy and Lactic Acidosis with Stroke like episodes) or Leigh's syndrome (Wallace D.C., 2005).

From a structural point of view, mitochondria are composed by two functionally different membranes: the plain outer membrane (OMM), contains high copy number of a specific channel, the Voltage Dependent Anion Channel (VDAC), which is able to forms pores on the membrane, becoming mostly permeable to ions and metabolites up to 5000 Da; the highly selective inner membrane (IMM), characterized by invaginations called *cristae* which enclose the mitochondria matrix. IMM is characterized by the presence of cardiolipin. In addition, on the IMM is it possible to find also other specific transport proteins. The space between the two membranes is called intermembrane space (IMS). The cristae define internal compartments formed by profound invaginations originating from narrow tubular structures called *cristae junctions* (Mannella et al., 2006) that limit the diffusion of molecules from the intra-cristae space towards the IMS, thus creating a micro-environment where the mitochondrial Electron Transport Chain (mETC) complexes are hosted and other proteins are protected from random diffusion. mETC consists of five different protein complexes: complex I (NADH dehydrogenase), complex II (succinate dehydrogenase), complex III

(ubiquinol cytochrome c reductase), complex IV (cytochrome c oxidase) and complex V that constitutes the F_1F_0-ATP synthase. Electrons are transferred from NADH and $FADH_2$ through these complexes to molecular oxygen: as electrons move along the respiratory chain, energy is stored as an electrochemical gradient across the inner membrane, thus creating a negative mitochondrial membrane potential (that is around -180mV against the cytosol). H^+ are forced to re-enter into the matrix mainly through complex V, which couples this proton driving force to the phosphorylation of ADP into ATP, according to the chemiosmotic theory. ATP is then released to IMS through the electrogenic Adenine Nucleotide Translocase (ANT), which exchanges ATP with ADP to provide new substrate for ATP synthesis. Finally, ATP can easily escape the IMS thanks to the mitochondrial porin of the outer mitochondrial membrane VDAC (Duchen, 2004).

Mitochondrial Ca^{2+} signaling

Mitochondria are important modulators of the amplitude and duration of Ca^{2+} signaling; they are able to accumulate a large amount of Ca^{2+} thanks to the electrochemical gradient established by the translocation of protons across the inner mitochondrial membrane (IMM), which is expressed as a membrane potential difference ($\Delta\Psi m$) of -180mV (negative inside) under physiological conditions (Mitchell, 1966). However, in resting conditions the mitochondrial calcium concentration is very low, comparable to the cytosolic one. In addition, experiments carried out in isolated mitochondria revealed that organelle Ca^{2+} transport has an apparent low affinity for this cation, that activates only at supraphysiological extramitochondrial [Ca^{2+}]. Thus, the role of mitochondria in Ca^{2+} homeostasis was considered marginal (i.e. limited to conditions of cellular Ca^{2+} overload), till the development of specific and reliable probes that directly reported major swings of mitochondrial [Ca^{2+}] even upon physiological stimuli (Rizzuto et al., 1992). The generation of photoprotein aequorin probe targeted to mitochondria allowed to demonstrate that in living and intact Hela cells the transient increase of [Ca^{2+}]cyt to 1-3μM, induced by physiological stimuli, is always associated with a parallel increase in [Ca^{2+}] in mitochondrial matrix which in most of cells reaches about 60-80 μM. It was thus clear that mitochondria play an active role in Ca^{2+} signaling. However, the chemiosmotic theory is not sufficient to explain the ability of energized mitochondria to rapid accumulate a large amount of Ca^{2+}: a lot of

experiments in isolated mitochondria have demonstrated that the systems of mitochondrial calcium accumulation are low affinity, they are activated when the $[Ca^{2+}]$cyt reaches value in order of 5-10µM, which rarely happens in physiological conditions. This discrepancy was resolved by the demonstration that the key of the rapid Ca^{2+}mit accumulation resides in the strategic location of mitochondria in close proximity to ER-resident Ca^{2+} channels and implies the assembly of a dedicated signaling unit at the interface of the two organelles. By labelling mitochondria and ER with targeted spectral variants of GFP (mtGFP and erGFP) the presence of overlapping regions of the two organelles, called "ER/mitochondria contact sites" has been revealed and the area of the contact sites has been estimated as 5-20% of the total mitochondrial surface (Rizzuto et al., 1998). In this way mitochondria are located in close proximity to the Ca^{2+} channels eliciting the Ca^{2+} rise (i.e. the IP_3 or RyRs receptors in the ER/SR or different classes of channels on the plasma membrane such us voltage- and store-operated channels) that is sufficient to stimulated the rapid accumulation of this cation. The idea of local Ca^{2+} microdomains between the mitochondria and the ER, was further demonstrated by Hajnoczky et al., and Rizzuto et al., by fast single-cell imaging of $[Ca^{2+}]$mit with targeted Ca^{2+}-sensitive GFPs (pericams and cameleons), which showed that $[Ca^{2+}]$mit increases originate from a discrete number of ER-sites and then rapidly diffuse through the mitochondrial network.

On the other hand, Ca^{2+} is extruded from the mitochondria by either a Na^{+}/Ca^{2+} exchanger (mNCX) and a H^{+}/Ca^{2+} exchanger (mHCX) expressed mainly in excitable and non-excitable tissue, respectively.

The existence of a sophisticated machinery for Ca^{2+} handling supported the general consensus that mitochondria could actively and rapidly change their $[Ca^{2+}]$ and participate in cellular homeostasis (Patron et al., 2013).

Mitochondrial Ca^{2+} Uniporter Complex: molecular identity and regulation

Through the years, there has been a broad consensus that the key molecule that allow mitochondria to rapid accumulate a large amount of Ca^{2+} across the ion-impermeable inner channel is the electrophoretic pathway called MCU (Mitochondrial Calcium Uniporter). Before the recent discovery in 2011, several candidates have been proposed but all these

studies have been ineffective or identified putative channels that still wait experimental confirmations. In 2007, Graier's group proposed that the isoforms 2 and 3 of the uncoupling protein UCP might be essential components of the uniporter machinery, but these data were not confirmed by other groups. Another research was performed by Clapham and coworkers who proposed Letm1 (leucine zipper EF-hand-containing transmembrane protein 1) as a H^+/Ca^{2+} antiport. This result is until known a matter of debate because in contrast with previous results identifying this protein as a K^+/H^+ exchanger and in contrast with the established properties of Na^+/Ca^{2+} (NCX) and H^+/Ca^{2+} (HCX) antiporters. Letm1 appeared to be sensitive to the MCU inhibitor ruthenium red (RuR) and the best characterized antiporter inhibitor CGP37157 and not reduces Ca^{2+} accumulation.

The best strategy for the identification of the molecular identity of MCU took advantage of a genome-wide approach. In 2008, Mootha and co-workers reported a mitochondrial "genoteque" called MitoCarta. It was obtained by performing mass spectrometry analyses, on both highly purified and crude mitochondrial preparations, from 14 different mouse tissues, in order to discover genuine mitochondrial proteins, further validated by GFP tagging (Pagliarini et al., 2008). By considering only those proteins localized in the IMM, expressed in the majority of mammalian tissues and with homologues in vertebrates and kinetoplastids (but not in yeast), they identified a protein named "Mitochondrial Calcium Uptake 1" (MICU1). MICU1 is a 54kDa protein possesses one transmembrane domain and two canonical EF-hands, essential for Ca^{2+}-sensing. However, the presence of only one putative transmembrane domain made it unlike that it can function as a Ca^{2+} channel. MICU1 was thus recognized as a modulator of the Mitochondrial Calcium Uniporter (MCU) (Perocchi et al., 2010).

The MitoCarta database and the discovery of MICU1 were the base for the subsequently discover of MCU. Our group screened *in silico* the MitoCarta database with the following parameters: i) ubiquitous expression in mammalian tissue, ii) minimal sequence requirements for channels (i.e. the existence of two or more transmembrane domains (TMDs), iii) absence in *S.cerevisia*, iv) presence in those organism in which mitochondrial Ca^{2+} transport with the properties of MCU was reported. Eventually, our and Mootha's labs identified a protein, encoded by the CCDC109A gene, which satisfies all the requirements of the *bona fide* Mitochondrial Calcium Uniporter (Baughman et al., 2011; De Stefani et al.,

2011). It was demonstrated that MCU localized to the inner mitochondrial membrane and its overexpression in Hela cells strongly increases the [Ca^{2+}]mit while its down regulation drastically reduces it without affecting classical mitochondrial properties (i.e. organelle shape, ER-mitochondria contact sites, ATP synthesis, O_2 consumption and ΔΨ). De Stefani et al. demonstrated that MCU is necessary and sufficient to mediate mitochondrial Ca^{2+} uptake. Indeed, purified MCU formed a RuR-sensitive channel in planar lipid bilayers.

Mitochondrial Potassium Channels

The strict control of inner mitochondrial membrane permeability is vital for efficient ATP synthesis. Conversely, increased mitochondrial membrane permeability due to activation of mitochondrial megachannels is a hallmark of cell death (Szewczyk A. et al., 2009). Within this context, potassium transport via ion channels seems to be an important mechanism to control the integrity of inner mitochondrial membrane. In this way potassium channels have been proposed to play a central role in triggering cardio- and neuro- protection (Szewczyk A. and Marban, 1999; O'Rourke, 2004). The electrogenic transport of potassium ions into the mitochondrial matrix is strictly ion channel dependent and, accordingly, it looks like to plasma membrane ion channel activity. The basic biophysical properties of mitochondrial inner membrane potassium channels including ATP-regulated potassium (*mitoK$_{ATP}$*) channels (Inoue I. et al., 1991), large-conductance Ca^{2+} activated potassium (*mitoBK$_{Ca}$*) channels (Siemen D. et al., 1999), voltage-dependent potassium (*mitoKv 1.3*) channels (Szabo I. et al., 2005) and *twin-pore TASK-3* potassium channels (Rusznàk Z. et al., 2008) have been found to be similar to some potassium channels present in the plasma membrane of various cell types. Potassium channels in the inner mitochondrial membrane must be regulated in subtle ways to avoid collapse of the membrane potential (Szewczyk A. et al., 2009).

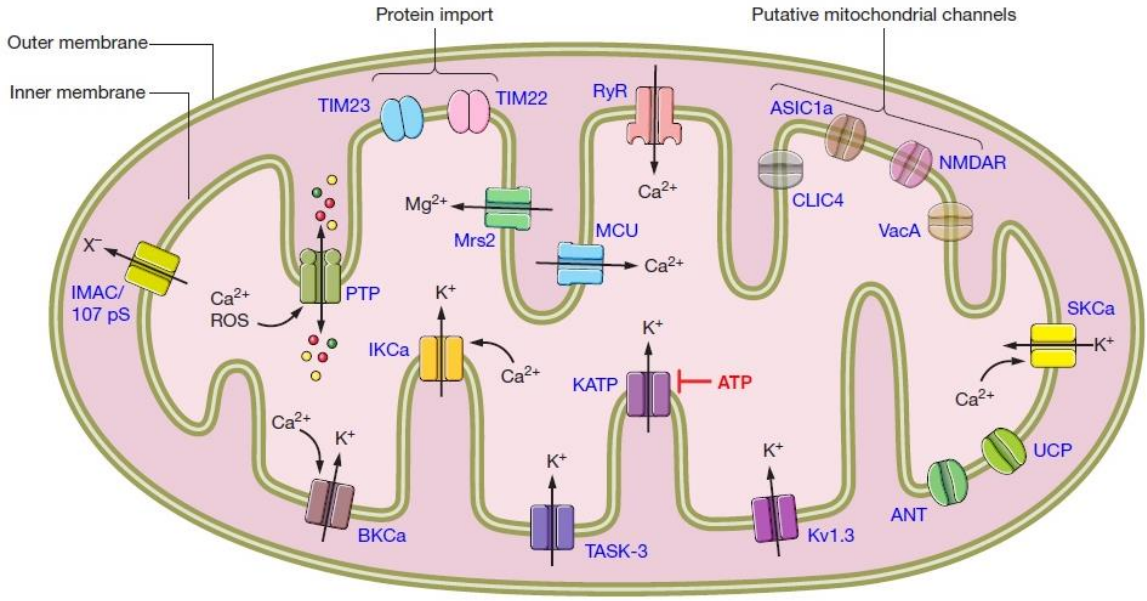

Fig.1. Overview of all electrophysiological activities in the IMM.

The Mitochondrial Potassium Cycle

Mitochondria are complex organelles. As reported in the general framework, they are composed by two different membranes, the outer mitochondrial membrane (OMM) and the inner mitochondrial membrane (IMM). The inner membrane contains the essential components of the electron transport proteins that transform the energy of substrate oxidation into an electrogenic proton efflux. The chemiosmotic theory, postulated by Peter Mitchell, is the basis for understanding the mitochondrial potassium cycle.

K^+ is the major monovalent cation in the cytoplasm (~150mM) and is consequently an important ion mediating changes in mitochondria volume when the K^+ conductance of the inner membrane is altered. The high negative electrical membrane potential, generating by protons ejection trough the electron transport system, drives an electrophoretic K^+ influx. Mitochondrial ATP-sensitive K^+ channels (called mitoK_{ATP}) also allow the diffusion of K^+ inside the mitochondrial matrix. Net uptake of K^+ salts is accompanied by osmotically obligated water, permeating through mitochondrial aquaporins, resulting in matrix swelling. Excess matrix K^+ is then exported by the electroneutral K^+/H^+ antiporter, which uses the energy stored in the proton gradient to export K^+ from the matrix (Fig.2).

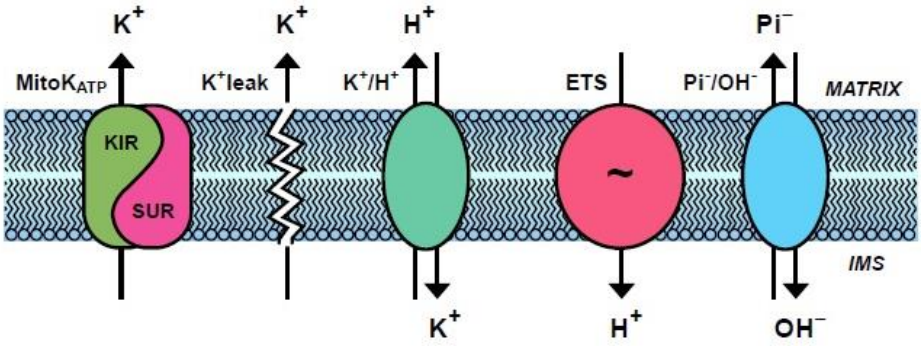

Fig.2. The mitochondrial potassium cycle.

The mitochondrial potassium cycle could be mimic in respiring mitochondria by the simultaneous use of two substances: ionophore valinomycin, which allows the rapid electrophoretic uptake of K^+, causes massive mitochondrial matrix swelling, but the addition of nigericin, which promotes the electroneutral exchange of H^+ and K^+, is able to prevent swelling but causes permeant depolarization and "uncoupling" (i.e. electron transport through components of the respiratory chain is not anymore coupled to ATP production). In intact mitochondria, energy dissipation is limited by the fact that channels and electrophoretic uptake pathways are strictly regulated. The so-called K^+ cycle thus can potentially modulate the tightness of coupling between respiration and ATP synthesis, thereby maintaining a balance between energy supply and demand in the cell and controlling the magnitude of the $\Delta\psi$ and ΔpH.

From the literature, it is reported that potassium transport plays three distinct roles in mitochondria: i) volume homeostasis in order to prevent excess matrix swelling, that is essential for maintaining the structural integrity of the organelle. This function is mediated by the K^+/H^+ antiporter and was first proposed by Peter Mitchell; ii) volume homeostasis in order to prevent excess matrix contraction, function that maintains an expanded matrix when K^+ influx diffuses inside the organelle. Maintaining matrix volume under these conditions is important because matrix contraction inhibits electron transport and also perturbates the structure-function of the intermembrane space (IMS). This volume regulation is mediated by the mitochondrial ATP sensitive K^+ channels ($mitoK_{ATP}$); iii) cell signaling functions to protect the cell from ischemia-reperfusion injury. This function depends on the ability of $mitoK_{ATP}$ opening to trigger increased mitochondrial production of

reactive oxygen species (ROS). The increased ROS levels activate a variety of kinases involved in the signaling pathways of cardioprotection.

The mitochondrial ATP sensitive potassium channels

The mitochondrial K_{ATP} channels (mitoK_{ATP}), namely its very existence, its composition, properties, regulation, functions and physiological and medical relevance, constitute the most controversial topic in the field of mitochondria channels. MitoK_{ATP} channel was initially described in liver mitochondria (Inoue I. et al., 1991). Later, it was also identified in heart, brain, kidney, skeletal muscle, human T lymphocytes and amoeba mitochondria. In 1980 and in 1988, two different laboratories tried to reconstitute a specific K^+ uniporter, and this was reported by Mironova et al. and Diwan et al. They identified channel activity corresponding to an inner membrane protein of 53-57kDa but they weren't able to obtain the exactly amino acid sequence. The channel was K^+-selective but its regulation was not characterized. Only in 1991, Inoue and co-workers provided unequivocal evidence for the existence of K^+ uniporters in the inner mitochondrial membrane by patch-clamping fused giant mitoplasts from rat liver mitochondria. They found the K^+ uniport was inhibited by ATP and glyburide, and named these mitochondrial ATP-sensitive K^+ channels (mitoK_{ATP}). Their work was followed by the purification and reconstitution of mitoK_{ATP} channels by Garlid's group, an experimental setup that allowed detailed studies of the regulatory properties of this channel. Garlid's group observed that mitoK_{ATP} exhibits many properties similar to those of the plasma membrane K_{ATP} channel.

The plasma membrane K_{ATP} channel (pmK_{ATP}) act as an important sensor of the cellular metabolic/energetic state, closing when energy (ATP) is abundant, and opening when the cell is "starved". pmK_{ATP} were first identified as 80pS channels by Noma in 1983 by experiments of patch clamping in cardiac myocytes (A. Noma., 1983), subsequently they have been found in many other cell types. For example, in pancreatic ß-cells pmK_{ATP} channels regulate glucose-stimulated insulin secretion and are the targets for sulfonylureas used to treat type 2 diabetes (F.M Ashcroft et al., 1999); in vascular smooth muscle they regulate vascular tone and in skeletal muscle, pmK_{ATP} may be active in fatigue (N.W.Davis et al., 1991). In cardiac muscle, they were originally thought to be involved in ischemic preconditioning and ischemic protection (G.J.Grover et al., 1989). From molecular point of

view, K_{ATP} channels are heterooligomers composed by a tetramer of ~40kDa Kir potassium channel-forming monomers associated with four regulatory sulfonylurea receptor (SUR)~160kDa subunits in an octameric complex. “Kir” stands for “K^+-selective inward rectifier” and the name “inward rectification” is due to voltage-dependent block by cytoplasmic Mg^{2+} or polyamines. ATP-sensitive channels are formed by the members of the Kir6 group, which comprises Kir6.1 and Kir6.2. These “core” channels have an inhibitory ATP binding site, which can be modulates by phospholipids. Sulfonylurea receptors (SURs) are members of the family of ATP binding cassette (ABC) transporters. ABC transporters have been classified into seven subfamilies. The ones involved in the formation of K_{ATP} channels belong to the ABCC/MRP subfamily, which includes also, e.g., the cystic fibrosis transmembrane conductance regulator (CFTR). In this case, SUR do not act as “pumps”, and their function seems to be essentially that of regulating K_{ATP} channel activity. Each SUR monomer has three transmembrane domains (TMD0-2) and two cytoplasmic nucleotide binding folds (NBFs), each composed of a Walker A and B domain separated by a linker region- that come together to generate two interacting site that can bind MgATP/MgADP. Involvement of these sites promotes activity of the channel and induces the state of closure. Mutating the lysine in Walker A or the aspartate in Walker B in either of the NBDs of SUR causes loss of MgADP activation of the channel (Nichols C.G. et al., 1996). The major SUR forms are SUR1 with high affinity for sulfonylurea, SUR2A (cardiac) and SUR2B (smooth muscle) with lower affinity for sulfonylurea. These are the proteins generally considered to partner with Kir6.x in the formation of pmK_{ATP} channels. For both Kir6.x and SURs, the expression of one or the other form is organ-and cell-type specific and different forms of heterocomplexes may coexist in the same cell (Fig.3).

Tissue	Composition
Pancreatic β-cell	Kir6.2-SUR1
Most, but not all, central neurons	
Mouse dentate gyrus granule cells	
Heart (ventricular)	Kir6.2-SUR2A
(Other heart tissues express also Kir6.1 and SUR1)	
Skeletal muscle	Kir6.2-SUR2A (but also other SURs, depending on muscle type/age)
Nonvascular smooth muscle and portal vein (portal vein also has Kir6.1/SUR2B)	Kir6.2-SUR2B
Vascular smooth muscle (KNDP)	Kir6.1-SUR2B (KNDP)
Mouse colon smooth muscle	
Guinea pig stomach smooth muscle cells	(Kir6.2 mRNA also found)
Hippocampus neurons	Kir6.1-SUR1
Frog retinal Mueller glial cells	
Neonatal heart (atrial)	Possibly heteromeric (all subunits found by PCR)

Fig.3. Tissue-dependent molecular composition of plasmamembrane K_{ATP} channels.

The molecular composition of mammalian mitoK_{ATP} channel is a debated matter. A large consensus supports the idea that mitoK_{ATP} appears to be qualitatively similar to the pmK_{ATP} channel counterpart. The first important evidence about the molecular structure was with Garlid's group that partially purified a mitochondrial fraction with mitoK_{ATP} channel activity (inhibited by ATP and activated by diazoxide) that contains, among several other proteins, 55 and 63kDa components. They proposed that the 63kDa protein in the fraction is the sulfonylurea binding subunit (mitoSUR) and the 55kDa is the pore forming unit of the channel (mitoKir). However, the identity of these protein remain elusive and until know is not clear who are the proteins that composed the molecular structure of mitoK_{ATP} channel.

An important role has been assigned to mitoK_{ATP}, especially in the heart, in protection from I/R injury, preconditioning and post conditioning. The process of ischemic preconditioning (IPC) was first described by Murry and coworkers in 1986 (Murry et al., 1986). IPC refers to a phenomenon in which brief episodes of hypoxia provide protection against a subsequent more prolonged period of ischemia (Murry et al., 1986; Kloner et al., 1998; Cohen et al., 2000). This protection includes a reduction in both infarct size and the incidence of cardiac arrhythmias. The belief that a mitoK_{ATP} acts as crucial element has probably influenced their tracing and the interpretation of some of the observations. Diazoxide, considered as a specific mitoK_{ATP} opener, was reported to protect mitochondrial functionality during ischemia. Garlid's group also showed that ATP-sensitive K^+ flux in mitochondria could be

inhibited by 5-HD, a know inhibitor of pmK_{ATP}. In figure 4 is reported a table about the modulators of pmK_{ATP} and $mitoK_{ATP}$ channel.

	$mitoK_{ATP}$	$mitoK_{ATP}$ and surface K_{ATP}	Surface K_{ATP}
Openers	Diazoxide Nicorandil BMS-180448 BMS-191095	Cromakalim Pinacidil P-1060 Sildenafil Isoflurane EMD60480 Aprikalim	P-1075[1] MCC-134[2]
Blockers	5-HD MCC-134	Glibenclamide	HMR1098 (1833) Glimepiride[3]

Fig.4. Modulators of K_{ATP} channels and their selectivity toward mitochondrial and surface channels.

It is unclear how the opening of a K^+ channel in the mitochondria would lead to cardioprotection. However, three hypotheses have emerged to explain the link between $mitoK_{ATP}$ channel opening and cardioprotection: (1) a decrease in the mitochondrial Ca^{2+} uptake, (2) swelling of the mitochondrial matrix and changes in ATP synthesis, and (3) changes in the levels of reactive oxygen species (ROS). Regarding the first hypothesis, diazoxide has been shown to reduce the mitochondrial Ca^{2+} uptake, and the effect can be reversed by 5-HD (Holmuhamedov et al., 1999). This change in mitochondrial Ca^{2+} uptake is thought to be mediated by a partial depolarization of $\Delta\Psi$ in response to $mitoK_{ATP}$ opening. Murata et al., 2011 showed that opening of $mitoK_{ATP}$ induces a reduction of Ca^{2+} accumulation in the mitochondria during simulated ischemia reperfusion. Regarding the second hypothesis, it has been known for some time that the opening of $mitoK_{ATP}$ causes mitochondrial matrix swelling, and that this in turn activates the respiratory chain providing more ATP to support the recovering myocardium (Halestrap, 1989; Grover and Garlid, 2000; O'Rourke, 2000). Garlid's group proposed that matrix swelling may lead to a more optimal contact between membrane proteins on the inner and outer membranes of the mitochondria, which may induce to an increase in ADP transport and ATP synthesis. About the third hypothesis, the ROS generated during the preconditioning period is thought to be protective (Vanden Hoek et al., 1989; Pain et al., 2000; Forbes et al., 2001). However, the ROS that is produced during reperfusion causes cell death (Ozcan et al., 2002). It is thought that the opening of $mitoK_{ATP}$ results in an increase in the protective ROS produced during

preconditioning phase and a decrease in the levels of ROS- generated during reperfusion phase (O'Rourke., 2004). In summary, the exact physiological role of mitoK_{ATP} and the mechanism of its involvement in cardioprotection will be proven only following its definitive molecular identification.

Calcium-dependent potassium channels

Two types of calcium-activated potassium channels have been described in various cell types: mitoBK_{Ca} (Big conductance potassium channel) and mitoIK_{Ca} (Intermediate conductance channel). Planar lipid bilayer experiments and direct patch clamping of mitoplasts of mammalian cells show that mitoBK_{Ca} channel has a conductance of 100-300ps (Skalska J. et al., 2008). The channel has been identified in glioma cell line as well as in ventricular cells, rat skeletal muscle and brain (Skalska et al., 2009). Evidence for its presence in mitochondria has also been provided by Western blot, electron microscopy and immunofluorescence microscopy. The channel is activated by micromolar concentrations of calcium and by the drugs 12,14-dichlorodehydroabietic acid (diCl-DHAA), NS1619 and NS11021, CGS7181, and CGS7184. It is blocked by specific inhibitors such as charybdotoxin, iberiotoxin and paxilline (Heinen et al., 2007). Concerning the molecular nature of mitoBK_{Ca}, it seems quite similar with that of the pmBK_{Ca}. MitoBK_{Ca} has been proposed to be activated under pathophysiological conditions that increase mitochondrial Ca^{2+} uptake, thus preventing excessive mitochondrial Ca^{2+} accumulation (by partially depolarizing the IMM, the driving force for calcium influx is reduced) and may also play a physiological role to fine-tune mitochondrial volume and/or Ca^{2+} accumulation under condition of, e.g. increased cardiac workload. Opening of mitoBK_{Ca}, similarly to mitoK_{ATP}, has been reported to protect against damage to the heart and other organs caused by ischemia and reperfusion. The protective effect of BK_{Ca} openers has been attributed to increased matrix K^+ uptake and volume, improved respiratory control, inhibition of mitochondrial Ca^{2+} overload and prevention of permeability transition pore (PTP) opening (Cheng Y. et al 2008). Opening of BK_{Ca} in isolated brain mitochondria was shown to inhibit ROS production by respiratory chain complex I and was hypothesized to be beneficial for neuronal survival.

MitoIK_{Ca} has been recently observed by patch clamping mitoplasts isolated from human colon carcinoma cells (De Marchi U. et al., 2009) but it is reported in other cell types such as

in Hela of human cervix adenocarcinoma origin and in mouse embryonic fibroblasts (Sassi N. et al., 2010). The channel is selectively inhibited by clotrimazole and TRAM-34. The biophysical and pharmacological properties of the mitoIK$_{Ca}$ and of the pmIK$_{Ca}$ channels of the same cells are indistinguishable, and the molecular weights of the IKs in the two membranes are the same (Sassi N. et al., 2010). MitoIK$_{Ca}$ may have a protective role similar to that proposed for mitoBK$_{Ca}$ and mitoK$_{ATP}$ channels; however, its physiological role has not been studied in detail so far.

Mitochondrial Kv1.3 potassium channel

Kv1.3 is a highly selective channel expressed in the plasma membrane of various cells. It plays a crucial role in the regulation of proliferation in lymphocytes (Cahalan M.D., Chandy K.G., 2009) as well in other cell types. Its presence in the mitochondria (mitoKv1.3) has been reported in T lymphocytes, macrophages, hippocampal neurons and presynaptic neurons, using patch clamp and/or immunochemistry. The molecular identification of the mitochondrial channel was obtained thanks to specific inhibitors margatoxin, and ShK and to a genetic model consisting in Kv1.3 KO CTLL-2 and CTLL-2 stably expressing Kv1.3 (Szabo I., et al 2005). Interestingly, the channel described in the mitochondria of hippocampal neurons by patch clamp displayed a different conductance with respect to the one found in lymphocytes, but both channels were sensitive to margatoxin. While pmKv1.3 activation is associated with cell proliferation (Cahalan M.D., Chandy K.G., 2009), its mitochondrial counterpart has been found to play a role in cell death. Concerning the mechanism, mitoKv1.3 was identified as a novel target of the pro-apoptotic Bcl-2 family protein, Bax and a physical interaction between the two proteins was shown to occur, but only in apoptotic cells. Recombinant Bax inhibited Kv1.3 channel activity with an efficiency similar to that observed to for the specific toxin inhibitors margatoxin or Shk. Incubating Kv1.3 positive isolated mitochondria with Bax or nanomolar concentrations of margatoxin or Shk -triggered apoptotic events, whereas mitoKv1.3 deficient mitochondria were resistant. The results indicated that during apoptosis, inhibition of IMM-located mitoKv1.3 by Bax leads to hyperpolarization, which results in the reduction of respiratory chain components and in enhanced production of ROS (Szabo I. et al., 2005). ROS is emerging as a key player in promoting cytochrome c release from mitochondria (Kaul S. et al., 2005). ROS are indeed

able to oxidase thiol groups and thus activate the PTP whose opening leads to depolarization and has been correlated to cytochrome c release. All these events, know to take place at mitochondria in various apoptotic models, were dependent on the presence of mitoKv1.3 and did not occur in mitochondria of Kv1.3- deficient CTLL-2/pJK cells. Whether mitoKv1.3 is the only channel of the Shaker voltage-gated potassium channel family located in mitochondria and whether its presence is obligatorily linked to its presence in the plasma membrane are still under investigation.

Two-pore potassium channel TASK-3

Recently TASK-3 (Twink-related acid-sensitive K^+ channel-3;KCNK9), a two-pore potassium channel know to reside in the plasma membrane, was identified in mitochondria of melanoma and keratinocyte cells by immunochemical and molecular biology methods (Rusznak Z. et al., 20008). In the pm, TASK-3 has a role in apoptosis and tumorigenesis (Patel A.J., Lazdunski et al., 2004). An investigation of the functional properties of the IMM TASK-3 channel by electrophysiology and/ or spectroscopic methods remains to be performed. Notably, a TASK-3 knock down melanoma cell line displays compromised mitochondrial function, suggesting that TASK-3 channels are functionally present in the mitochondria of the melanoma cells, and their function is essential for the survival of these cells (Kosztka L. et al., 2011).

Inward Rectifying Potassium Channel of the outer mitochondrial membrane

Although the outer membrane of mitochondria is widely accepted to be freely permeable to small ions due to the presence of the voltage-dependent anion channel, VDAC, a recent paper describes the discovery of an inwardly rectifying voltage-dependent potassium selective ion channel (Kir) in this membrane by patch clamp experiments (Fieni F. et al., 2010). The channel was regulated by osmolarity and cAMP and was found to be blocked by cesium. However, inhibition by other classical potassium channel inhibitors, TEA^+ and 4-amino-pyridine, was not achieved. The molecular nature of this channel as well as its single channel conductance remain to be clarified. Furthermore, further studies will need to exclude that this activity is related to a cationic subconductance state of VDAC or is the

result of a contamination by ER via the so-called mitochondria-associated endoplasmatic reticulum membranes (MAMs) (Hayashi T. et al., 2009).

AIM

In 2011, the long searched mitochondrial calcium uniporter (MCU) was finally identified. MCU is a 40kDa protein with two transmembrane domains and is sufficient to reconstitute Ruthenium Red-sensitive Ca^{2+}-selective channel activity *in vitro*. The availability of this molecular information opened the molecular era of mitochondrial Ca^{2+} signaling (De Stefani et al., 2011). When I started my PhD project, the original goal was to identify novel MCU interactors. Indeed, an *in silico* analysis revealed a strong potential candidate, namely coil-coiled domain 51 (CCDC51). Similarly to MCU, CCDC51 is a widely expressed gene, conserved among vertebrates and encoding for a protein with two transmembrane domains. However, the structure and function of CCDC51 were never investigated before. We thus started to study this protein in order to test whether it could modulate mitochondrial Ca^{2+} accumulation. Although its overexpression causes profound changes in organelle Ca^{2+} homeostasis, we soon realized that CCDC51 was not a direct regulator of the MCU complex. Nonetheless, the effect triggered by CCDC51 overexpression was so fascinating that we decided to fully dissect its function. In particular, we reasoned that the effects triggered by CCDC51 overexpression could be explained through an increase of cation permeability of the inner mitochondrial membrane. We wondered whether CCDC51 could be act as an ion channel per se. We here identify a mitochondria localized protein complex that mediates ATP-sensitive potassium currents, the so-called mitoK$_{ATP}$. Similarly to its plasma membrane counterpart, the mitoK$_{ATP}$ is formed by a pore-forming subunit, named mitoK (previously known as CCDC51), and an ATP-sensitive subunit, named mitoSUR (previously known as ABCB8). The new goal of my research is to elucidate the precise molecular composition, as well as the physiological role of the mitoK$_{ATP}$ *in vitro*.

RESULTS

1. In silico analysis

The Mitochondrial Calcium Uniporter (MCU) is the Ca^{2+} channel of the inner mitochondrial membrane required for rapid Ca^{2+} accumulation inside organelle matrix. I started this project with the original goal to identify new MCU modulators by performing an *in silico* screening of putative MCU interactors. We thus performed a bioinformatics analysis looking for all the proteins fulfilling the following criteria:

- Mitochondrial localization
- With no homologues in *Saccharomyces cerevisiae*
- With at least one transmembrane domain
- Possessing at least one coiled-coil domain, structural motifs that proteins use to interact with other proteins or to form oligomers.

We obtained a list of 10 proteins that includes Ccdc90a, Ccdc90b, Chchd1, Chchd2, Chchd3, Chchd4, Chchd7, Ccdc58, Ccdc44 and Ccdc51. Most of these proteins are already characterized in the literature, but one of them, encoded by the CCDC51 gene (NCBI gene ID 79714), is completely uncharacterized. The gene that codifies CCDC51 is located on the short arm of chromosome 3 in humans, while in mice is on chromosome 9. Functional predictions based on primary amino acidic sequence show the presence of two transmembrane domains (Fig.1A).

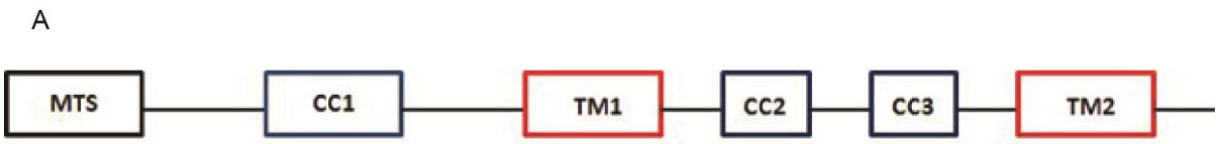

Fig.1A. ***CCDC51 includes two transmembrane domain.*** *Schematic representation of the predicted domains in the CCDC51 protein.*

CCDC51 is a protein of unknown functions, since there are no papers in the literature investigating its physiopathological role. We thus started looking to its function by testing CCDC51 as a putative regulator of the mitochondrial Ca^{2+} channel MCU.

2. Real-time PCR analysis

We performed real-time PCR analysis of mouse tissue (mRNA extraction and real-time PCR was performed as described in the Methods section). Tissue expression profiling showed ubiquitous presence in all investigated tissue (Fig.2A), suggesting that CCDC51 could play a widespread housekeeping role in all cells, similarly to MCU.

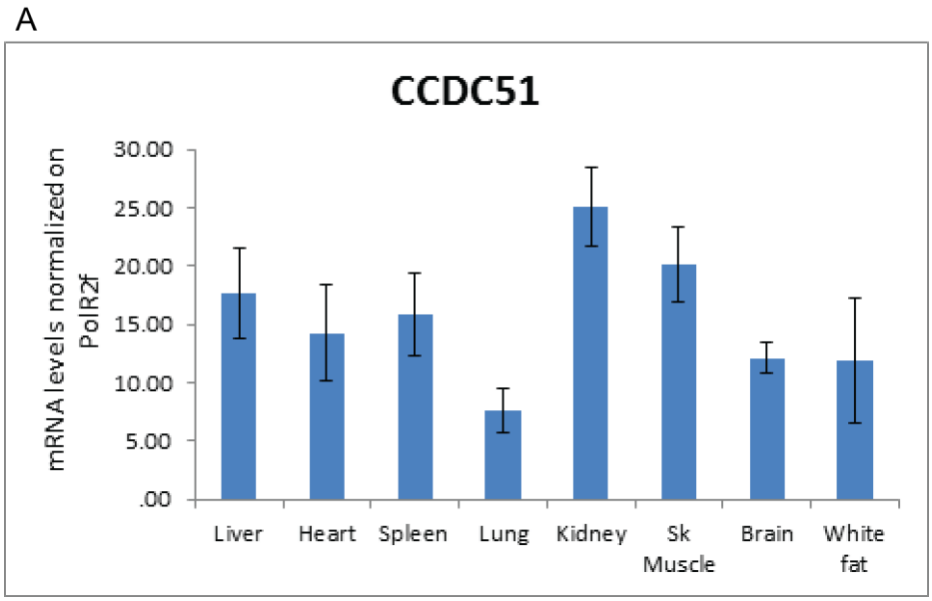

Fig.2A. ***CCDC51 is ubiquitously expressed in mouse tissues****. Real-time PCR analysis of mouse tissues. mRNA extraction and real-time PCR was performed as described in the Methods section. Expression levels are normalized to PolR2f.*

CCDC51 expression levels correlate with those of MCU, except for skeletal muscle, lungs and brain (Fig.2B): this data can in principle support the hypothesis of CCDC51 as a regulator of the Mitochondrial Calcium Uniporter.

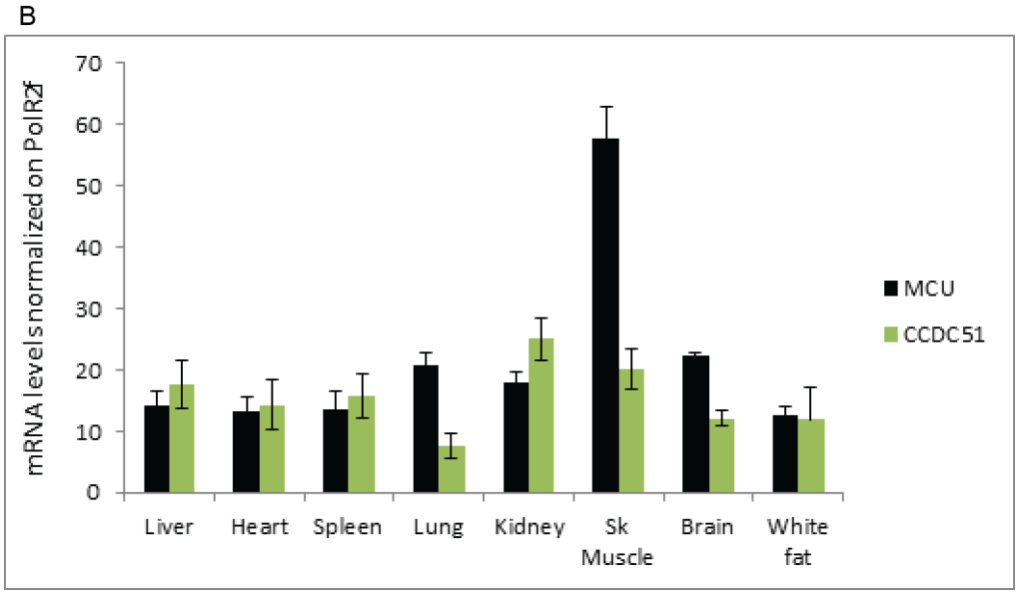

Fig.2B. ***CCDC51 is ubiquitously expressed in mouse tissues, similarly to MCU****. Real-time PCR analysis of mouse tissue. mRNA extraction and real-time PCR was performed as described in the Methods section. Expression levels are normalized to PolR2f.*

3. Biochemical characterization

- *3.1 Localization and topology*

First, we looked to the localization of the endogenous protein by fixing Hela cells and marking them with primary antibody capable of recognizing and displaying CCDC51 protein

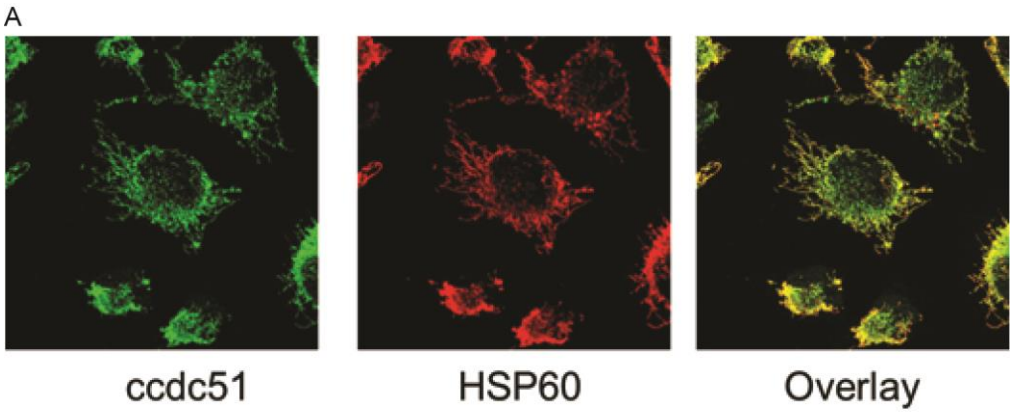

Fig.3.1A. ***Endogenous CCDC51 localize to mitochondria.*** *Hela cells were fixed and immunocytochemistry was performed with α-CCDC51 and α-HSP60 antibodies followed by incubation with Alexa488, Alexa555 conjugated secondary antibodies as described in the Methods. Representative confocal images are shown.*

with fluorescent secondary antibody conjugated with AlexaFluor488. Immunofluorescence staining showed full co-localization with mitochondria marker HSP60 conjugated to AlexaFluor555 (Fig.3.1A).

Then, in order to better study the functional role of CCDC51, we cloned and expressed the protein in Hela cells. We analyzed the localization of the overexpressed protein compared the subcellular distribution of endogenous CCDC51, by co-expressing tagged version of CCDC51 (CCDC51-**GFP** and CCDC51-**Flag**) and proteins that are able to localize at the level of mitochondria (i.e. mtRFP or HSP60) and carrying out immunofluorescence. Hela cells were transiently co-transfected with mtRFP, in order to mark mitochondria, and CCDC51 conjugated to GFP tag. After 36 hours of expression, by laser scanning confocal microscopy (LSCM) mitochondria have been identified mtRFP by exciting at wavelength of 543nm, while the CCDC51-GFP protein was excited at 488nm. Confocal images showed a complete overlap of the two emitted fluorescence, supporting the mitochondrial distribution of CCDC51 (Fig.3.1B).

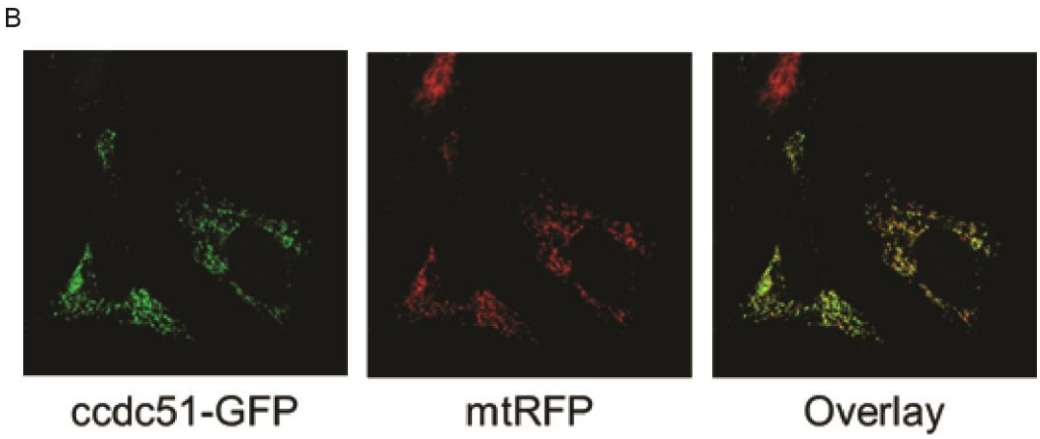

Fig.3.1B. ***CCDC51-GFP localizes to mitochondria****. Hela cells were transfected with CCDC51-GFP and mtRFP. After 36 hours the cells were fixed and representative confocal images are shown.*

This result was also confirmed by immunofluorescence staining of transfected Hela cells with CCDC51-Flag and mitochondrial marker HSP60 (Fig.3.1C).

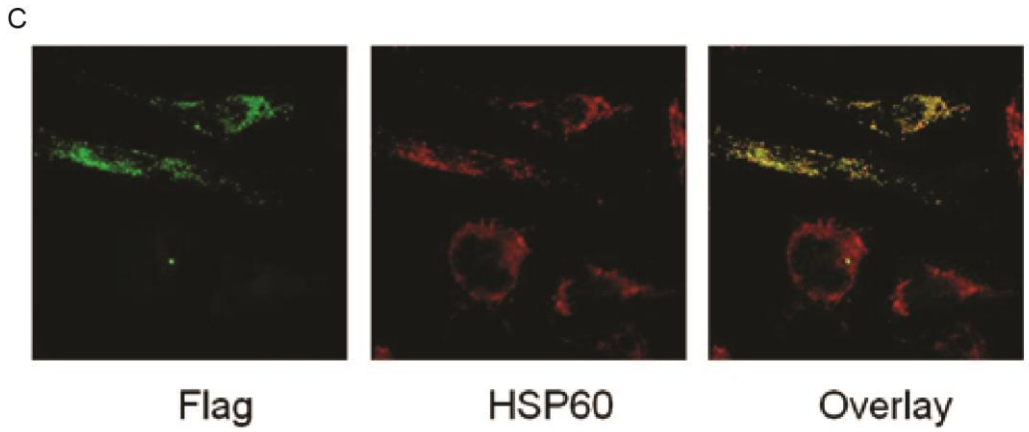

Fig.3.1C. ***CCDC51-Flag localizes to mitochondria****. Hela cells were transfected with CCDC51-Flag. After 36 hours the cells were fixed and immunocytochemistry was performed with α-Flag and α-HSP60 antibodies followed by incubation with AlexaFluor488, AlexaFluor555 conjugated secondary antibodies as described in Methods. Representative confocal images are shown.*

The membrane localization of CCDC51 was further evaluated in deeper detail by sub-cellular fractionation followed by mitochondrial sub-fractionation. Mouse liver tissue was homogenized with a Dounce homogenizer and centrifuged at 1000g (2300rpm) in order to separate entire cells and nuclei. The supernatant was then centrifuged at 7000g (9000rpm) to pellet the crude mitochondrial fraction. Mitoplasts, mitochondria lacking the outer mitochondria membrane, were obtained by osmotic swelling by incubating the mitochondrial fraction in 20mM HEPES for 20 min. Mitochondria and mitoplast fractions were then subjected to carbonate extraction. Na_2CO_3 is a salt that, following ultracentrifugation, allows to separate membrane protein from soluble ones. Western blot allowed us to identify the correct localization of CCDC51 at the level of mitochondria.

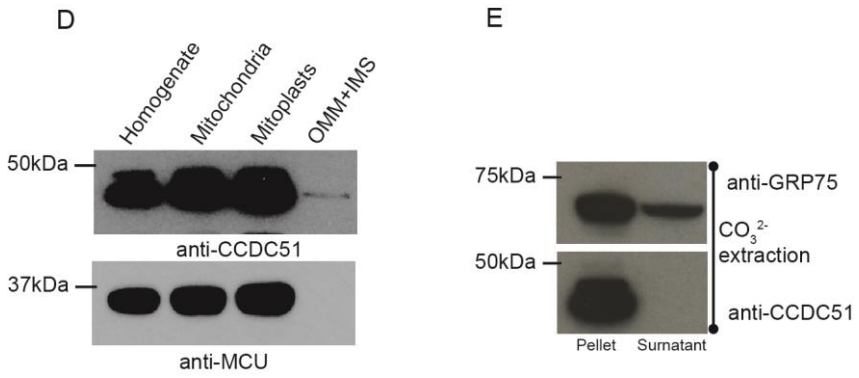

Fig.3.1 D-E. ***CCDC51 localizes at the inner mitochondrial membrane.*** *(D) Immunoblot analysis of CCDC51 in the indicated fractions obtained from mouse liver, using antibodies against MCU (inner mitochondrial membrane) and CCDC51. (E) Membranes (i.e. pellet) were extracted from isolated mitochondria and probed with the indicated antibodies.*

Western blot analysis showed that CCDC51 is enriched in mitochondria compared to the total homogenate, confirming immunofluorescence data that show CCDC51 is a mitochondrial protein. It is also further enriched in mitoplasts indicating that CCDC51 can be located either in the inner mitochondrial membrane or into the matrix (Fig.3.1D). In addition, Western blot analysis of carbonate extraction showed that CCDC51 is present exclusively in the pellet fraction (Fig. 3.1E), thus indicating that is an integral membrane protein. Taken together, these data indicate that CCDC51 is a membrane protein of the inner mitochondrial membrane.

In order to dissect the precise membrane topology, we took advantage of the availability of two different CCDC51 antibodies, one raised against the N-terminal, and the other covering the C-terminal, as indicated in figure 3.1G. We then performed a protease protection assay in isolated mitoplasts. In this method, proteinase K can access all proteins exposed outside the inner mitochondrial membrane. Conversely, all proteins residing inside the organelle are protected from enzymatic digestion. Proteinase K is used at the concentration of 100µg/ml and it is allowed to act at first for 10 min, then for 30 min. Enzymatic digestion is finally blocked with PMSF (phenylmethanesulfonyfluoride), a general inhibitor of serine proteases. In order to check the correct proteolytic activity of the protein, 1% Triton X100 is added to mitochondrial treated with proteinase K. Proteins are then loaded on SDS-PAGE and analyzed through Western blot.

As demonstrated by figure 3.1F, the antibody against $CCDC51_{N\text{-terminal}}$ revealed the appearance of a 25kDa band after treatment with Proteinase K for 10 and 30 minutes, while the 45kDa band (corresponding to the full length CCDC51 protein) is progressively reduced in intensity. This pattern indicates that Proteinase K has partially digested the protein, but a portion of CCDC51 remains protected (i.e. the band at approximately 25kDa). This indicate that region recognized by $CCDC51_{N\text{-terminal}}$ antibody is protected from proteinase K treatment, and thus resides inside organelle matrix. Conversely, the C-terminal region of the protein completely disappears after protein digestion, thus revealing its localization outside the organelle. As expected, in this experimental settings HSP60, a protein located inside mitochondrial matrix, is fully protected from Proteinase K digestion (Fig.3.1F-G).

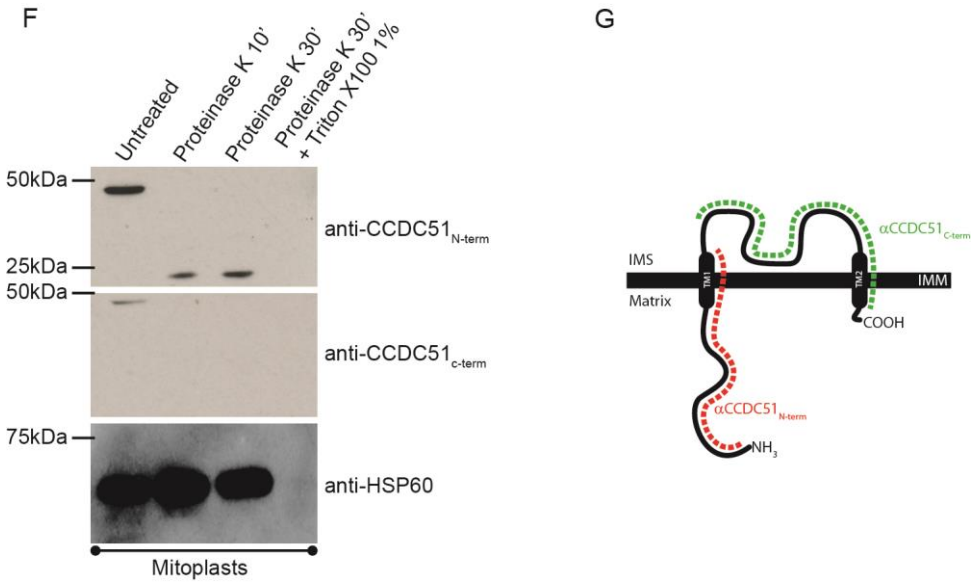

Fig.3.1F-G. ***Membrane topology of CCDC51***. (F) *Immunoblot analysis of mitoplasts from Hela cells and treated with proteinase K for the indicated time. These samples were probed using antibodies against* $CCDC51_{N\text{-term}}$, $CCDC51_{C\text{-term}}$ *and HSP60. (G) Schematic representation of CCDC51 organization and domains recognized by antibodies.*

- *3.2 FRET analysis*

In order to better understand the structure of the protein, we used a FRET-based assay to assess in situ protein-protein interactions.

For this purpose, a CCDC51-GFP (donor) and a CCDC51-mCherry (acceptor) chimera were generated and compared with two non-interacting fluorophores (GFP and mCherry). We confirmed the occurrence of FRET by monitoring fluorescence acceptor photobleaching. mCherry was bleached in a defined region with a 592nm high power laser and changes in CCDC51-GFP (excitation at 488nm) and CCDC51-mCherry (excitation at 543nm) fluorescence were measured. When FRET occurs, acceptor photobleaching leads to the de-quencing and consequent increase in donor fluorescence. Thus, FRET was calculated as the normalized increase in donor fluorescence after acceptor bleaching. Figure 3.2A shows a representative experiment. When CCDC51-GFP and CCDC51-mCherry were co-expressed, significant FRET could be detected (15,47% ± 6,2), whereas minimal FRET was detected when GFP and mCherry were not fused to CCDC51 (0%) (Fig.3.2B). The calculated efficiency is in line with other reports using the same FRET pair (Goh et al., 2011; van der Krogt et al., 2008) and does not correlate with the expression level of the fluorescent proteins.

A

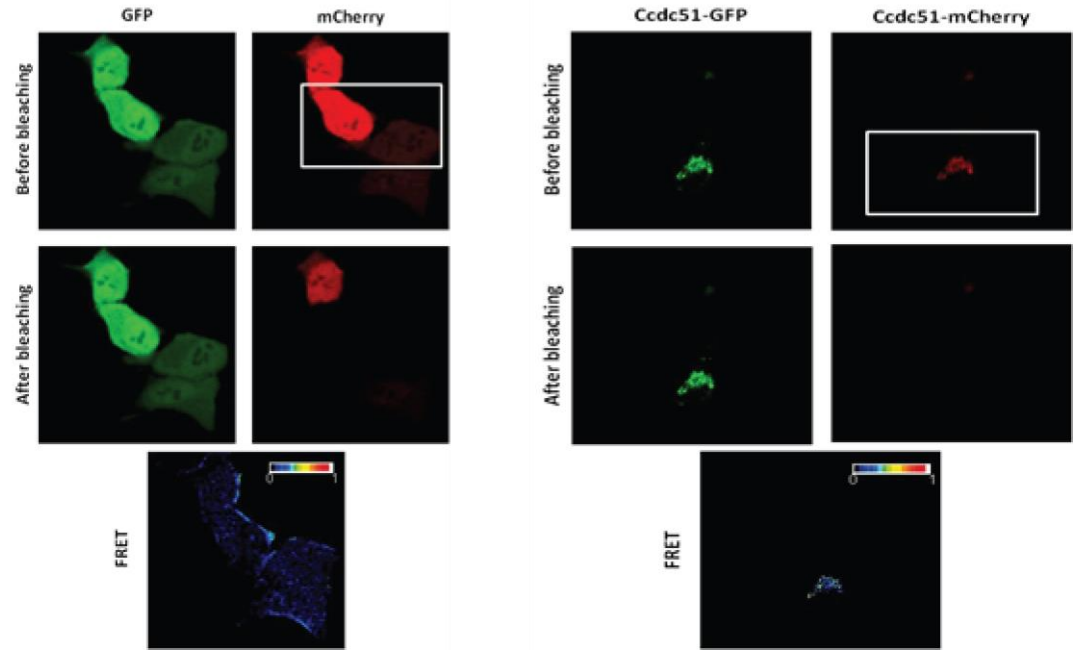

Fig.3.2A-B. ***CCDC51 forms oligomers in vivo***. (A) *Hela cells were transfected with GFP and mCherry or CCDC51-GFP and CCDC51-mCherry and analyzed after 24h. Images of donor and acceptor were taken before and after photobleaching of the indicated region (white box). FRET was calculated as detailed in the experimental procedures. (B) Histogram bar diagram shows FRET efficiency of the indicated donor and acceptor pairs.*

We used the MCU-GFP/MCU-mCherry pair as positive control, since they already known to interact and form oligomers. (Raffaello A., et al. 2013).

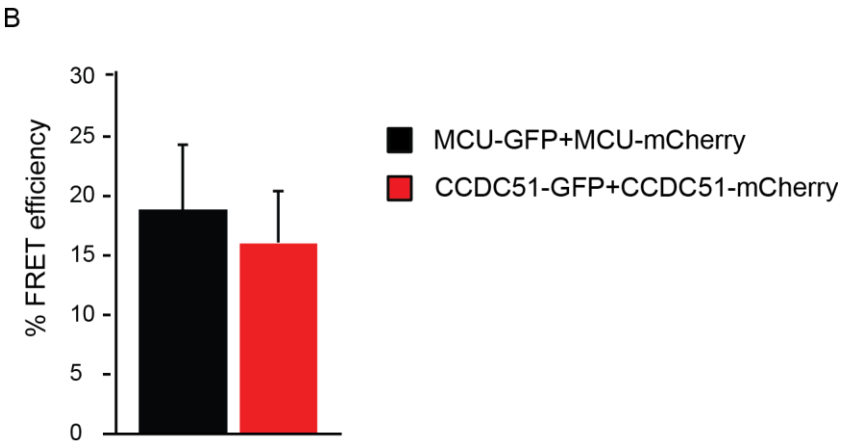

4. Effects of CCDC51 overexpression on mitochondrial functions

- *4.1 CCDC51 overexpression induces a drastic decrease of mitochondrial calcium uptake*

In order to test the hypothesis that CCDC51 could be a possible modulator of MCU, we verified the role of CCDC51 in mitochondrial Ca^{2+} handling. Ca^{2+} measurements were then carried out with aequorin-based-mitochondrial and cytosolic Ca^{2+} probes (mtAEQ and cytAEQ).

CCDC51 overexpressing (CCDC51-V5 and CCDC51-GFP) and control Hela cells were perfused with modified Krebs-Ringer buffer supplemented with 1mM $CaCl_2$ (KRB) and were challenged, where indicated, with 100µM histamine, an inositol 1,4,5-trisphosphate-generating agonist causing Ca^{2+} release from endoplasmic reticulum.

In control cells, the $[Ca^{2+}]$cyt rise evoked by histamine stimulation was ± 3,1µM. We can observe no differences in cytosolic calcium accumulation in CCDC51 overexpressing cells (± 3µM after 36h of transfection) (Fig. 4.1A-B).

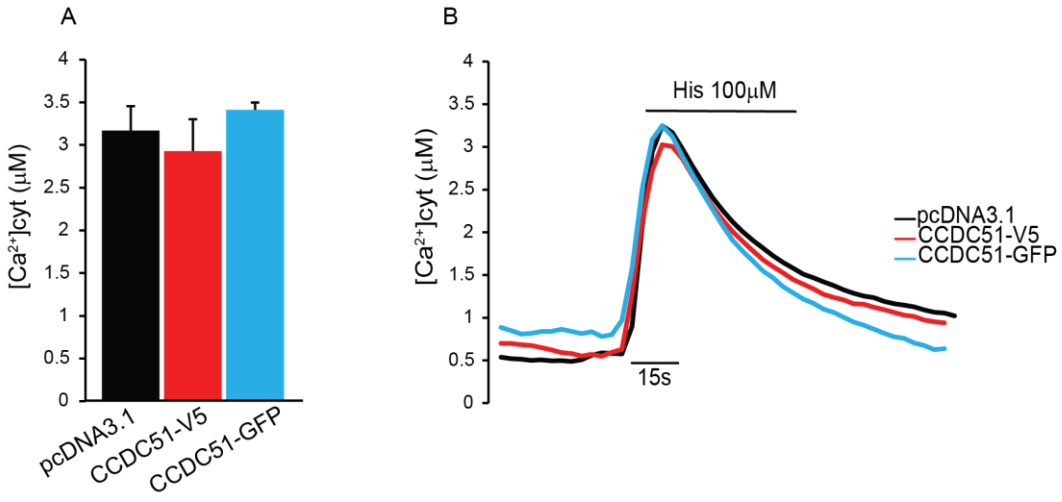

Fig.4.1A-B. ***CCDC51 overexpression does not change [Ca^{2+}]cyt in Hela cells****. Cells were transfected with pcDNA3.1 and CCDC51-V5 or CCDC51-GFP. After 36h, [Ca^{2+}]cyt uptake upon histamine stimulation was measured (n=6).*

These data indicate that the overexpression of CCDC51 in Hela cells does not affect the cytosolic calcium accumulation.

We then measured mitochondrial Ca^{2+} levels in these same experimental groups in order to evaluate if the protein CCDC51 has an effect in the regulation of mitochondrial calcium accumulation.

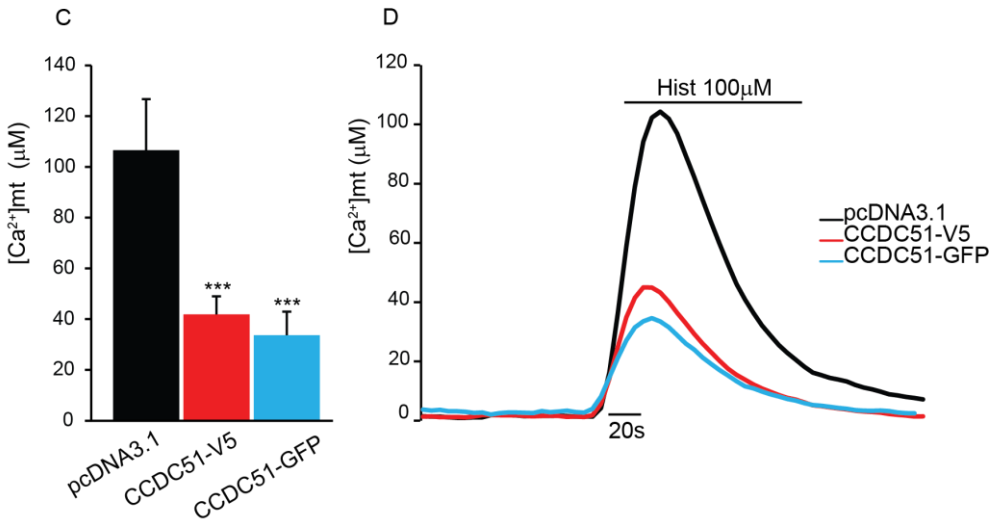

Fig.4.1C-D. ***CCDC51 overexpression critically reduces [Ca^{2+}]mt in Hela cells.*** *Cells were transfected with pcDNA3.1 and CCDC51-V5 or CCDC51-GFP. After 36h, [Ca^{2+}]mt uptake upon histamine stimulation was measured (n=6, ***p<0.001)*

Histamine stimulation shows that the overexpression of CCDC51 causes a drastic reduction in agonist- induced [Ca^{2+}]mt peak compared to control cells, supporting the notion that only mitochondria are affected (Fig.4.1C-D).

In order to selectively investigate the contribution of mitochondria Ca^{2+} machinery, we also measured mitochondrial calcium uptake in digitonin permeabilized cells. This experiment allows evaluating the properties of the mitochondrial Ca^{2+} uptake machinery independently of the ER Ca^{2+} release and the formation of microdomains of high [Ca^{2+}] in close proximity to mitochondrial calcium channel. Measurements in digitonin-permeabilizied cells are performed initially by perfusing cells with Intracellular Buffer (IB) for 60s. Cells are then perfused with the same buffer with 50µM digitonin for 60second, in order to permeabilized the plasmatic membrane, and washed with IB/EGTA buffer for other 60second. The mitochondrial [Ca^{2+}] rise is then triggered by perfusing digitonin-permeabilized cells with a solution containing 2 µM. Also in this experiment, overexpression of CCDC51 decreases the uptake rate (Fig.4.1E-F). Thus indicating that CCDC51 selectively impairs mitochondrial calcium accumulation.

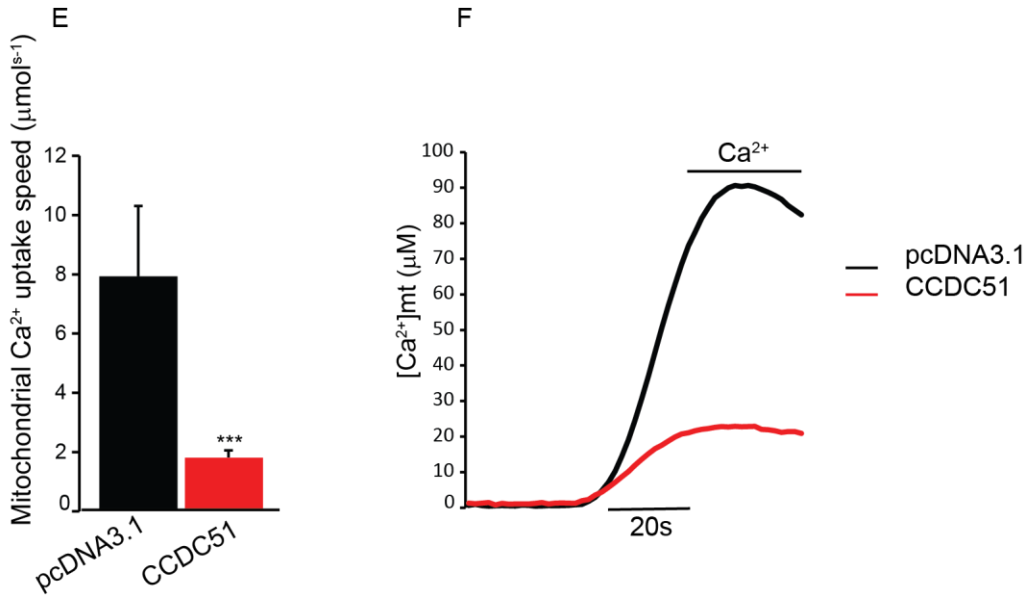

Fig.4.1E-F. ***CCDC51 overexpression critically reduces [Ca^{2+}]mt in Hela permeabilized cells****. Cells were transfected with pcDNA3.1 and CCDC51-V5. Experiment for valuate mitochondrial Ca^{2+} uptake in permeabilized cells were performed as described in Material and Method section.*

- *4.2 The overexpression of CCDC51 decreases mitochondrial calcium uptake irrespective of MCU levels*

In order to further test if CCDC51 could exert a role in the regulation of mitochondrial calcium accumulation by MCU, we overexpressed both proteins on Hela cells and we tested the mitochondria calcium accumulation with aequorin-based mitochondrial Ca^{2+} probes (mtAEQ).

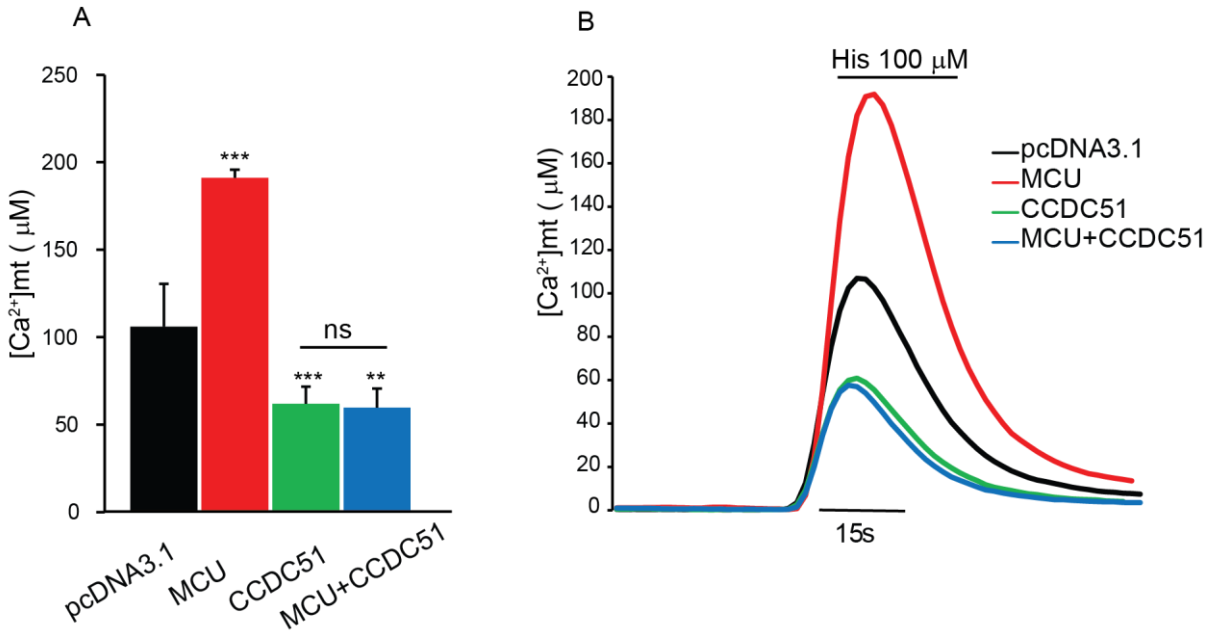

Fig.4.2A-B. ***CCDC51 overexpression critically reduces [Ca^{2+}]mt in the overexpression of MCU****. Hela cells were transfected with pcDNA3.1, MCU and CCDC51. After 36h, [Ca^{2+}]mt uptake upon histamine stimulation was measured (n=6,** p<0.05, ***p<0.001).*

MCU overexpression per se caused an increase in the [Ca^{2+}]mt rise (De Stefani et al., 2011), CCDC51 overexpression not only decreased the [Ca^{2+}]mt rise evoked by 100μM histamine, but markedly reduced it even when MCU is overexpressed together (Fig.4.2A-B). This suggests that the effect of CCDC51 is independent of the amount of the MCU in the cells, thus suggesting that CCDC51 is not a modulator of the uniporter.

- *4.3 CCDC51 is not an MCU interactor*

We looked for biochemical confirmation of the previous result by using the FRET technique in living cells. We generated and imaged different combinations of GFP- and mCherry-

tagged MCU and CCDC51 proteins respectively. FRET was evaluated by acceptor photobleaching, as described above. Representative fluorescence images of the MCU-GFP (donor) and CCDC51-mCherry (acceptor) pair are shown in figure 4.3A. No significant FRET was observed (2,4% ± 1,6) compared to positive control (MCU-GFP and MCU-mCherry) (Fig.4.3B), thus indicating the absence of direct interaction between MCU and CCDC51.

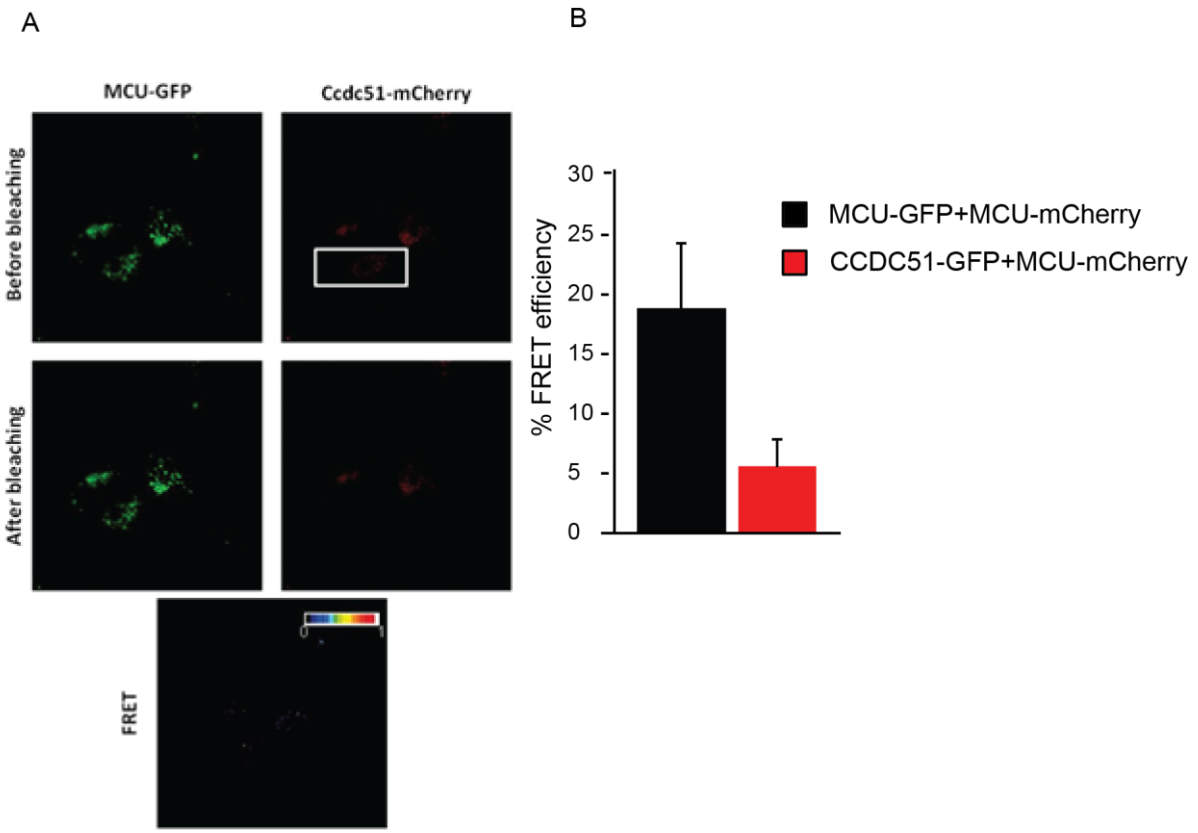

Fig.4.3A-B. ***CCDC51 and MCU do not interact in vivo****. Hela cells were transfected with MCU-GFP and CCDC51-mCherry and analyzed after 36h. Images of donor and acceptor were taken before and after photobleaching of the indicate region (white box). FRET was calculated as detailed in the experimental procedures. Histogram bar diagram shows FRET efficiency of the indicate donor and acceptor pairs.*

This data supports the idea that CCDC51 is not a modulator of MCU. After ruling out the possibility of a direct effect of CCDC51 on organelle Ca^{2+} uptake machinery, we started investigating other mitochondrial parameters that may justify the large decrease in mitochondrial calcium accumulation caused by CCDC51 overexpression.

- *4.4 CCDC51 overexpression induces a drastic decrease of mitochondrial membrane potential*

First, we tested the hypothesis that suppression of mitochondrial Ca^{2+} transients could be secondary to a decrease of mitochondrial membrane potential. It is indeed well known that the electrochemical potential (ΔΨ) is formed in energized mitochondria and it is composed by an electrical component (Δμ) and a proton concentration gradient (ΔpH). The mitochondrion-selective tetramethylrhodamine methyl-ester (TMRM) dye was used to measure the mitochondrial membrane potential. This compound is membrane-permeant cation, that easily distributes into various compartments according to their electrochemical gradient. The accumulation of TMRM in mitochondria is driven by their membrane potential (-150/-180mV). In order to avoid the self-quenching of the probe, cells are loaded with a low TMRM concentration (20nM). Changes in mitochondria membrane potential will result in differences in absolute fluorescence intensity. The specificity of the signal is verified by collapsing the ΔΨ through the treatment with the protonophore FCCP (10μM).
Hela cells were transfected with p-EGFP, as control, or CCDC51-GFP. 36 hours after transfection, cells were loaded with TMRM and left for 30 minutes at 37°C. Then, we acquired two images, one to discriminate transfected and untransfected, the other to measure the mitochondrial membrane potential. After the acquisition of a stable baseline, we added FCCP that induces the collapse of mitochondrial membrane potential and allowed us to calculate the residual fluorescence in the absence of potential.

As shown in figure 4.4, the overexpression of CCDC51-GFP protein caused a drastic decrease of mitochondria membrane potential compared to control cells, a result that can fully explain the reduction in mitochondria calcium accumulation.

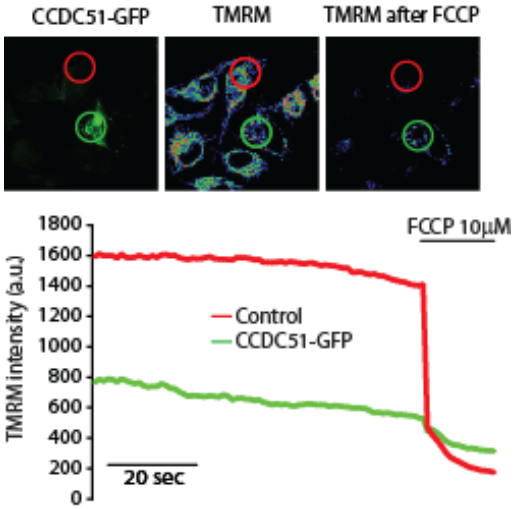

Fig.4.4. ***CCDC51 overexpression decreases mitochondrial membrane potential****. Hela cells were transfected with pEGFP or CCDC51-GFP. 36h after transfection, cells were loaded with tetramethylrhodamine (TMRM) and fluorescence was measured as described in Material and Methods section (n=6). Representative traces of one control and one CCDC51 overexpressing cells are shown.*

- *4.5 CCDC51 overexpression induces a disarrangement of cristae structure*

In order to further investigate the consequences of CCDC51 overexpression on mitochondrial structure and function, we analyzed mitochondrial ultrastructure through electron microscopy.

The mitochondrion is structurally defined by its two membranes: a limiting outer membrane that enwraps the energy-trasducing inner membrane, which in turn encloses a dense, protein-rich matrix. The outer membrane is topologically simple, varying in shape depending on whether the mitochondrion is in a cell (usually tubular when attached to the cytoskeleton, sometimes reticulated) or isolated in suspension (ellipsoidal or spherical). The inner membrae, which has a much large surface area than the outer membrane, contains features referred to as *cristae,* which have long been represented as simple infoldings of this membrane (Carmen A. Manella., 2006).

Hela cells were transfected with p-EGFP (as control) and CCDC51-GFP, and 36 hours after transfection cells were fixed and imaged through Transmission Electron Microscopy (TEM). Mitochondria usually form elongated structures in control cells. In CCDC51-GFP expressing cells, mitochondria became dot-like structures (Fig.4.5A).

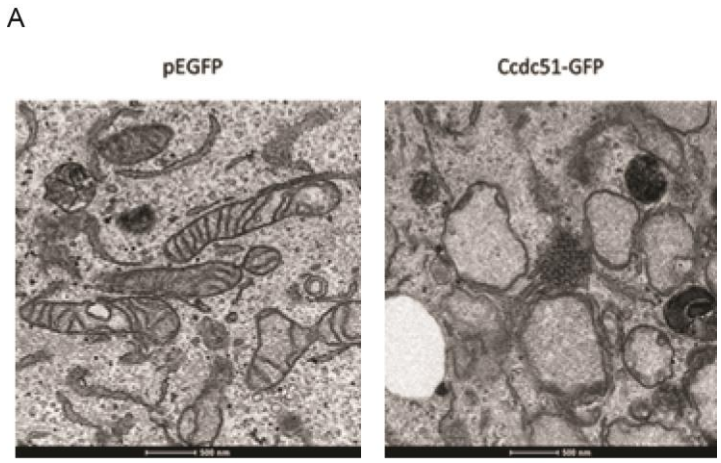

Fig.4.5A. ***CCDC51 overexpression leads to organelle fragmentation and swelling***. *Representative trasmission electron microscopy images of mitochondria in control and CCDC51 overexpressing Hela cells*.

TEM images showed that the overexpression of CCDC51-GFP protein induces a total collapse of cristae and mitochondria appears to be empty compared to control cells.

The experiments performed so far show that the overexpression of CCDC51 induces a decrease in mitochondrial calcium accumulation that is secondary to a substantial decrease of mitochondrial membrane potential. One potential explanation is that CCDC51 could be a component of the Permeability Transition Pore (PTP).

Indeed, opening of PTP pore increases ion permeability of the inner mitochondrial membrane, thus leading to organelle depolarization. PTP opening can be inhibited by cyclosporine A, which binds cyclophilin D, a peptidyl-prolyl cis-trans isomerase located in the mitochondrial matrix. In order to analize a possibile correlation between the PTP and CCDC51, Hela cells that overexpress CCDC51 protein were grown in the presence of cyclosporine (50μM) and the mitochondrial calcium uptake was measured with aequorin-based mitochondrial Ca^{2+} probes (mtAEQ).

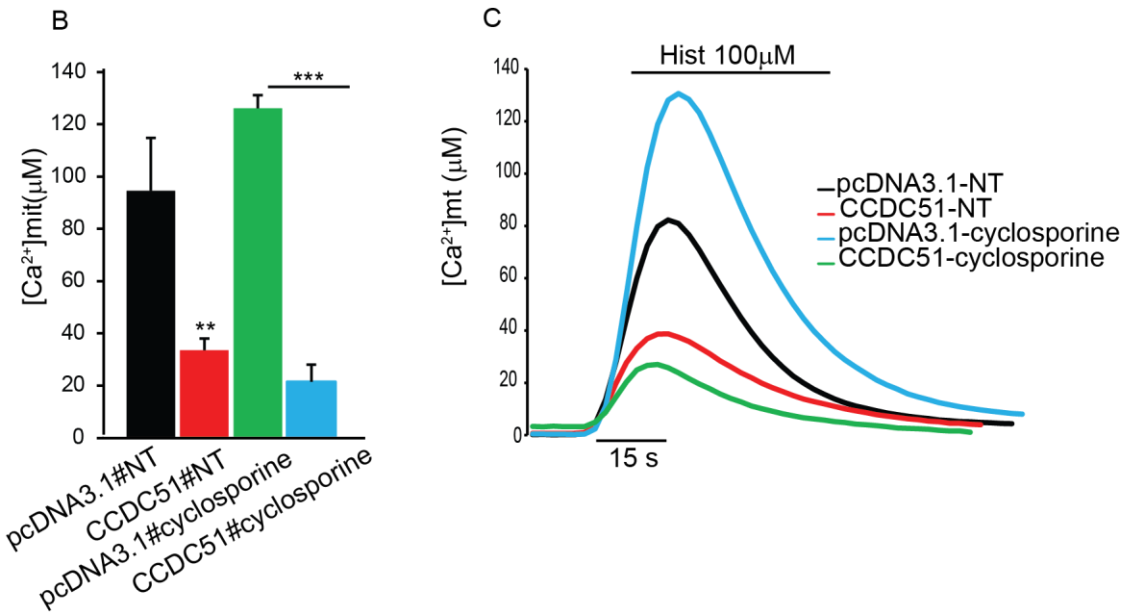

Fig.4.5B-C. ***CCDC51 is not a CsA-sensitive PTP component****. Hela cells were transfected with pcDNA3.1 and CCDC51 in the presence of cyclosporine A. After 36h, [Ca^{2+}]mit uptake upon histamine stimulation was measured (n=4,** p<0.05, ***p<0.001)*

As shown in figure 4.5B-C, CsA induces an increase of mitochondrial calcium uptake in control cells. This effect is in line with an increase of mitochondrial membrane potential caused by the inhibition of the transient opening on PTP. However, it is not the case for Hela cells that overexpressed CCDC51, where even in the presence of CsA we can observe a decrease of mitochondria calcium uptake. This result suggests that CCDC51 is not a component or a modulator of the PTP.

- *4.6 CCDC51 overexpression induces mitochondrial fragmentation*

Mitochondria are dynamic organelles that fuse and divide to form constantly changing tubular networks in all eukaryotic cells. Furthermore, regulation of mitochondrial dynamics is crucial for the health of the cells, because it is essential for cellular development and homeostasis, as well as apoptosis. The cytoplasmic dynamin-related GTPase DRP1 plays a key role in mitochondrial fission, while Mfn1, Mfn2 and Opa1 mediate organelle fusion.

In order to test if CCDC51 could be involved in mitochondria dynamics we analyzed mitochondrial morphology when the protein is overexpressed. Hela cells were transiently co-transfected with mtRFP and CCDC51. Confocal images clearly showed that the overexpression of CCDC51 induces mitochondrial fragmentation (Fig.4.6A).

A

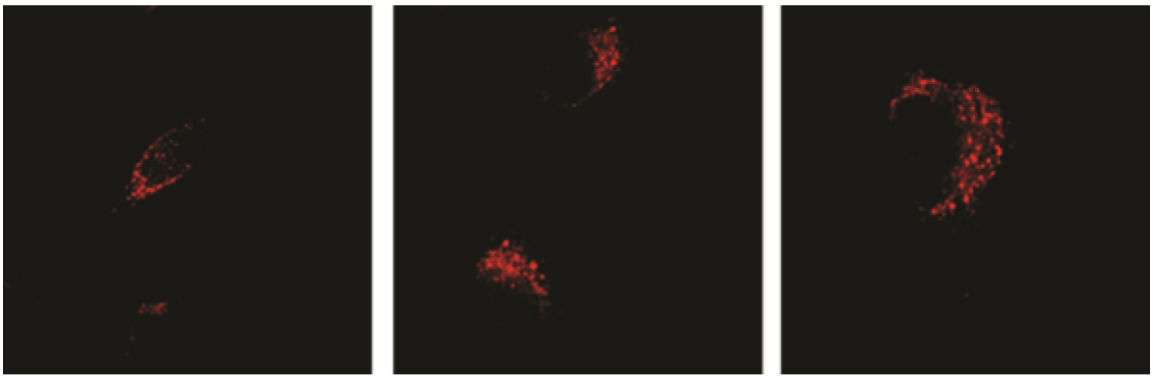

Fig.4.6A. ***CCDC51 overexpression leads mitochondrial fragmentation****. Hela cells were transfected with CCDC51 and mtRFP. 36 hours after transfection cells were fixed and representative confocal images are shown.*

CCDC51 overexpressing mitochondria appear as punctuate structures, suggesting either excessive mitochondrial fission or decreased organelle fusion. In order to further investigate a possible role of CCDC51 protein in this process, we analyzed mitochondria morphology after the overexpression of DRP1 (Dynamin-related protein 1) or its dominant negative form DRP1K38A, that inhibts the normal function of DRP1 thus leading to hyperfused mitochondria.

Hela cells were transiently co-transfected with mtRFP and CCDC51, together with DRP1 or DRP1K38A.

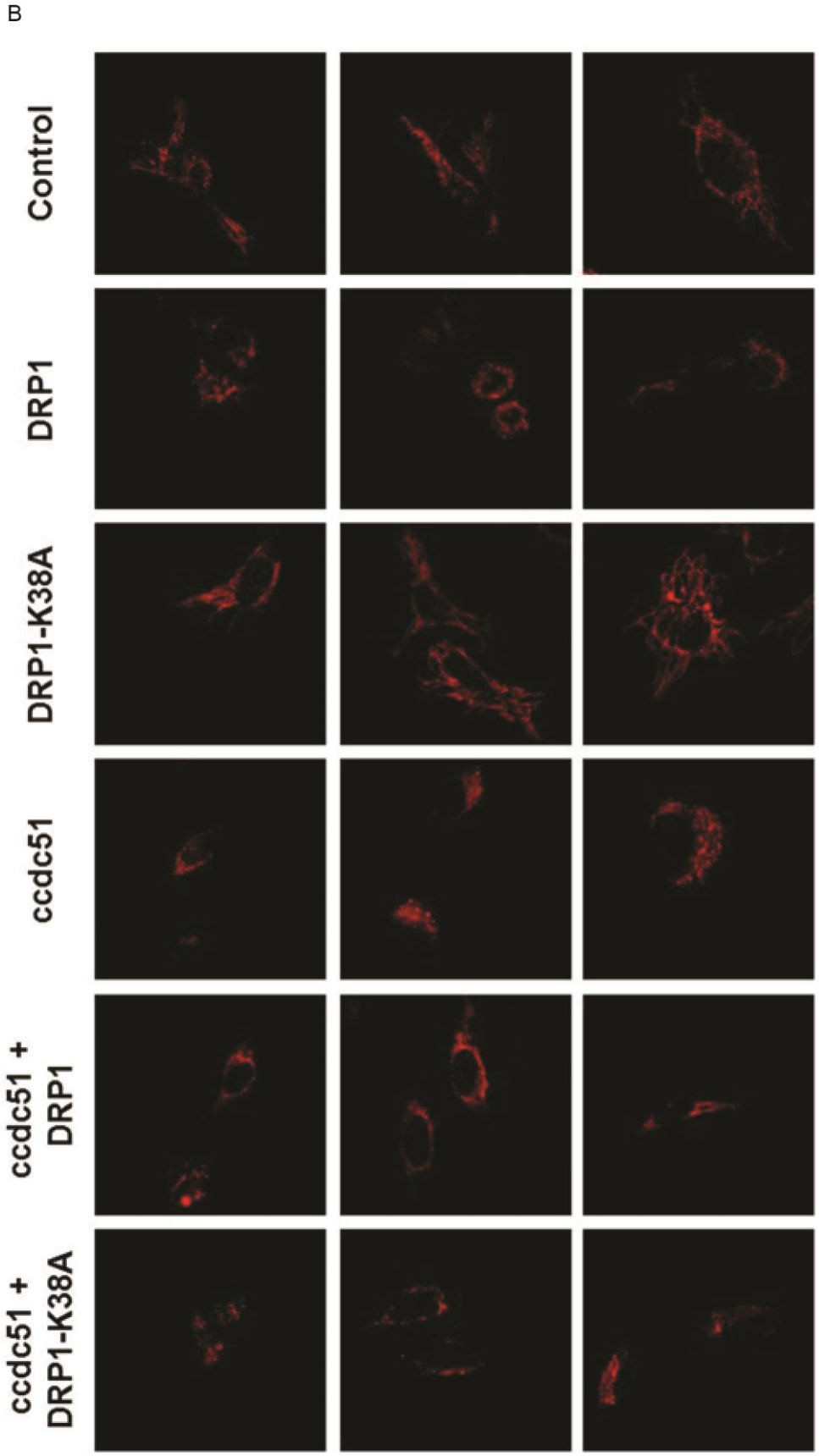

Fig.4.6B. ***CCDC51 is not involved in mitochondrial dynamics****. Hela cells were transiently transfected*

with CCDC51, DRP1, DRP1-K38A and mtRFP. After 36 hours the cells were fixed and representative confocal images are shown.

Confocal images showed that the overexpression of DRP1 and CCDC51 alone caused mitochondrial fragmentation. On the contrary, the overexpression of DRP1-K38A alone induced mitochondrial elongation. When CCDC51 is overexpressed together with DRP1 mitochondria were still obviously fragmented, with no major differences compared to cells overexpressing CCDC51 alone. Most importantly, mitochondria overexpressing both CCDC51 and DRP1-K38A appeared fragmented (Fig.6B). This result underlines how the inhibition of mitochondrial fission was not sufficient to restore the phenotype that induce the overexpression of CCDC51 alone, thus suggesting that CCDC51 and DRP1 act on different cellular processes.

Thus, these results suggest that CCDC51 is not directly implicated in mitochondrial fusion and fission dynamics.

5. CCDC51 is a potassium channel

CCDC51 overexpression leads to a major dysregulation of multiple mitochondrial parameters, including organelle fragmentation and swelling, loss of membrane potential and decrease of mitochondrial Ca^{2+} accomulation. All these effects can in principle be explained by an increase of cation permeability of the inner mitochondrial membrane. Indeed, similar effect can be mimicked by treatment with mitochondrial uncouplers, including valinomycin, a potassium ionophore (data not shown).

We thus wondered whether CCDC51 could act as an ion channel. We analyzed channel activity of the purified protein reconstituted in a planar lipid bilayer. For this purpose, a His-tagged CCDC51 construct was generated and expressed in a wheat-germ cell-free transcription/translation, where membrane contaminants are absent. The purified protein was inserted into lipid bilayers and its electrophysiological activity was assed in a medium containing 150mM KCl on both sides. In this experimental setup we observed a clear channel activity characterized by a conductance of 75pS. In addition, currents could be fully inhibited by tetraethylammonium (TEA) chloride, a general inhibitor of potassium channels (Fig.5A-B). these results indicate that CCDC51 is a potassium-permeant channel.

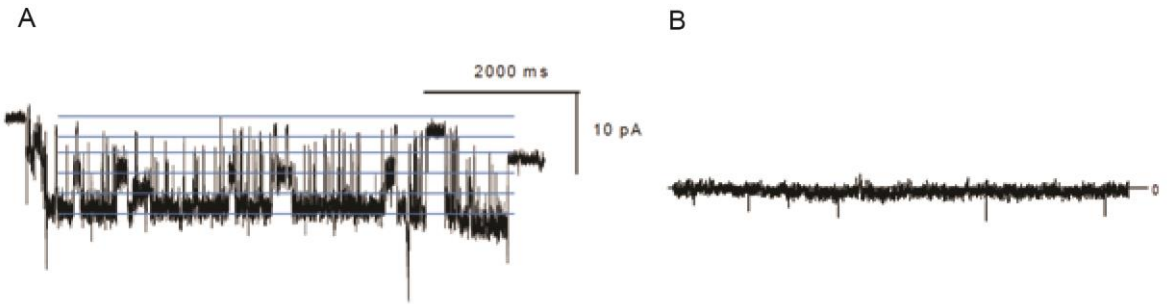

Fig.5A-B. ***Purified CCDC51 shows channel activity in lipid bilayers and it is inhibited by tetraethylammonium (TEA) chloride***. (A) *Electrophysiological recordings of purified CCDC51 in vitro and reconstituted in a planar lipid bilayers. (B) CCDC51 traces after addition of tetraethylammonium (TEA) chloride.*

We next wondered whether CCDC51 could be a part of the mitoK$_{ATP}$, given that all the other mitochondrial K^+ channels (mitoBK$_{Ca}$, two-pore doomain TASK-3 and mitoK$_v$1.3) were already identified.

ATP-sensitive potassium-selective channels (K$_{ATP}$) mainly exist on the plasma membrane of excitable cells (pmK$_{ATP}$), but they are reported to be present also in some intracellular organelles. The mitochondrial ATP-sensitive potassium channels (mitoK$_{ATP}$) is one of the most controversial topics in the field of mitochondrial research, since even its very existence is a matter of debate. MitoK$_{ATP}$ mediates the electrophoretic transport of potassium ions inside the organelle matrix, thanks to the large driving force represented by the mitochondrial membrane potential, and it is inhibited by normal physiological ATP concentrations. Although CCDC51 *per se* acts as ATP-insensitive (data not shown), we supposed that the ATP sensitivity could be conferred by a regulatory channel subunit, similary to what happens in pmK$_{ATP}$. Indeed, pmK$_{ATP}$ channels are heterooligomers composed by a tetramer of Kir (K^+-selective inward rectifier, i.e. the channel forming subunit) associated with four regulatory sulfonylurea receptor (SUR) subunits (belonging to the ABC superfamily), all arranged in an octomeric complex.

We thus looked to ATP-binding proteins of the inner mitochondrial membrane and we found at least one good candidate.

- *5.1 In silico analysis of ATP-binding proteins*

The ABC genes represent the largest family of transmembrane protein. Most of these proteins bind ATP and use the energy to drive the transport of various molecules across all cell membranes (Higgins 1992; Childs and Ling 1994; Dean and Allikmets 1995). Proteins are classified as ABC transporters based on the sequence and organization of their ATP-binding domains, also knows as nucleotide-binding fold (NBF). The NBFs contain characteristic motifs, Walker A and B, separated by <90-120 aminoacids, found in all ATP-binding proteins. The functional protein typically contains two NBFs and two transmembrane (TM) domains. The TM domains usually contain 6-11 membrane-spanning-helices. Four members of mitochondrial ABC system are already reported in literature. ABCB7, ABCB10 and ABCB8 are localized in the inner mitochondrial membrane, while ABCB6 is found in the outer mitochondrial membrane.

However, we started from all ABC proteins located in mitochondria according to MitoCarta database. We thus obtained a list of 12 proteins that includes Abcb1a, Abcb1b, Abcb4, Abcb5, Abcb6, Abcb7, Abcb8, Abcb9, Abcb10, Abcb11, Tap1 and Tap2. Among them, we first focused our attention to the mitochondrial protein ***ABCB8***. It is a half-molecule ABC protein that localizes to the inner mitochondrial membrane (Ardehali H. et al., 2005), and apparently contains a single transmembrane and nucleotide binding domain (Hogue D.L. et al., 1999). ABCB8 has been shown to protect against oxidant induced cell death (Ardehali H. et al., 2005), however its primary function is not known, although it was reported to be involved in mitochondrial iron transport (Yoshihiko Ichikawa et al., 2011). We prioritized this protein because it has the same tissue expression of CCDC51. In addition, mitochondria from ABCB8 knock out mouse hearts show disruption of cristae and deformed morphology.

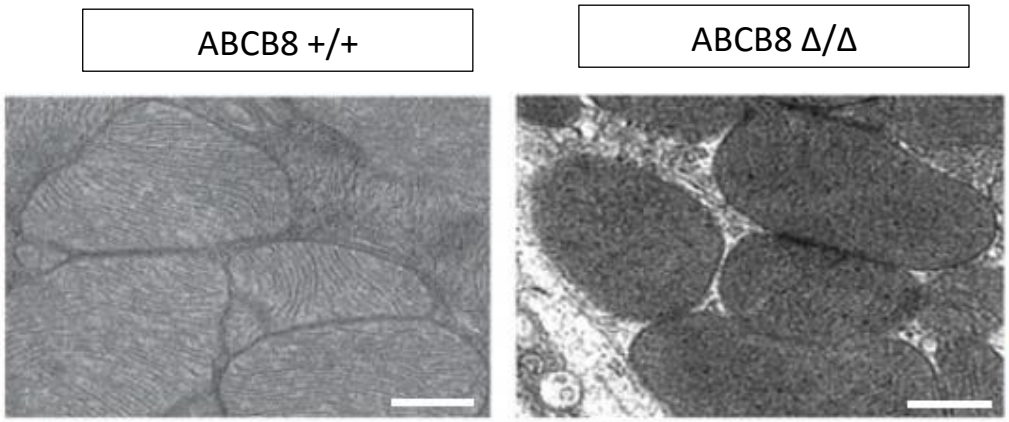

Figure shows TEM images of hearts from Abcb8+/+ and Abcb8 Δ/Δ mice. Hearts from Abcb8+/+ mice show well aligned mitochondria with clearly distinguishable cristae. Mitochondria from Abcb8 Δ/Δ mouse hearts show disruption of cristae and deformed morphology. This phenotype resembles what we observed when CCDC51 is overexpressed in Hela cells. We thus tested the physical and functional interactions between CCDC51 (called **mitoK** hereafter) and ABCB8 (called **mitoSUR** hereafter). According to our hypothesis, the concomitant overexpression of mitoK and mitoSUR should restore the mitochondrial dysfunction caused by the overexpression of mitoK alone, since mitoSUR confers the correct gating and closes the mitoK channel in normal physiological conditions.

6. Effects of mitoK and mitoSUR on mitochondrial functions

- *6.1 MitoK and mitoSUR physically interact*

In order to investigate if mitoK and mitoSUR interact each other, co-immunoprecipitation analysis was performed. Hela cells were co-transfected with mitoK-V5 and mitoSUR-Flag chimeras. 36 hours after transfection, the cells were lysed and immunoprecipitation was carried out using an α-Flag antibody as bait. When mitoK and mitoSUR were co-expressed, the α-Flag antibody immunoprecipitated mitoK, thus revealing the interaction (Fig.6.1).

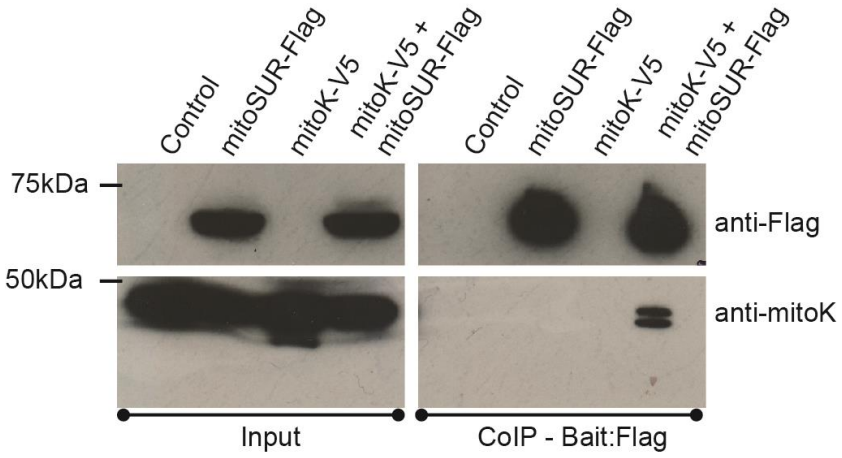

Fig.6.1. ***MitoK physically interacts with mitoSUR****. Hela cells were transfected with the indicated constructs. Flag-tagged mitoSUR was immunoprecipitated from cells extract with a specific α-Flag antibody. The precipitated proteins were immunoblotted with α-Flag and α-mitoK antibodies.*

- *6.2 Effects of the co-expression of mitoK and mitoSUR on mitochondria calcium uptake*

In order to test if the physical interaction between mitoK and mitoSUR has a functional effect, we analyzed how the concomitant overexpression of the two proteins could affect mitochondrial Ca^{2+} responses. Ca^{2+} measurements were then carried out with aequorin-based-mitochondrial Ca^{2+} probes (mtAEQ).

As shown in figure 6.2A-B,overexpression of mitoK alone causes a significant decrease of mitochondrial calcium uptake after histamine stimulation. Conversely, the overexpression of the mitoSUR subunit alone does not affect organelle Ca^{2+} responses. Most importantly, the concomitant overexpression of the two subunits perfectly rescue mitochondrial Ca^{2+} dynamics, suggesting the restoration of mitochondrial membrane potential and consequently of the proper physiological channel activity.

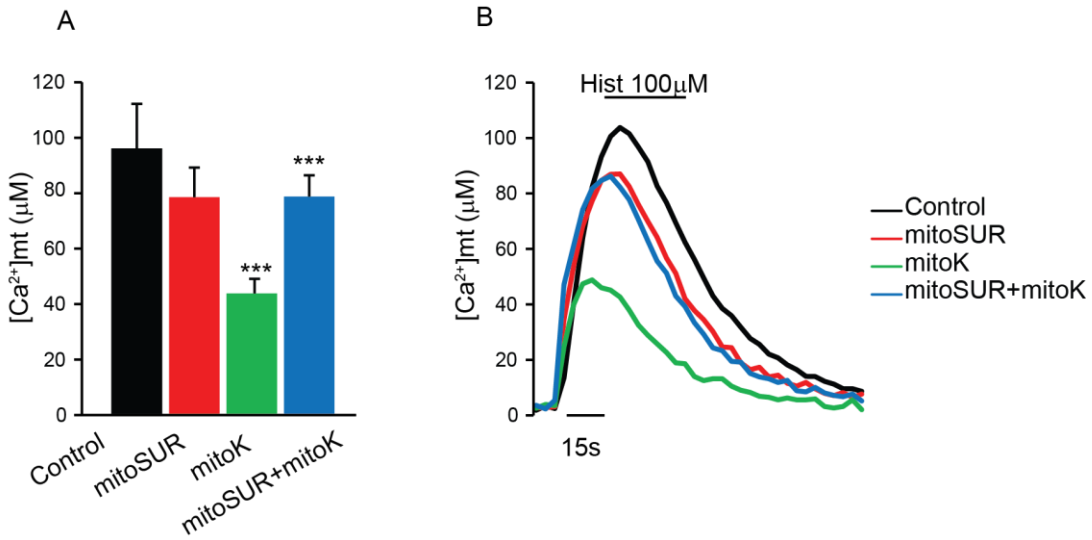

Fig.6.2A-B. ***MitoSUR inhibits mitoK channel activity****. Hela cells were transfected with the indicated constructs together with mitochondrial-targeted aequorin probe and agonist induced peaks of matrix [Ca^{2+}] was measured (n=6, ***p < 0.001)*

- *6.3 Effects of co-expression of mitoK and mitoSUR on mitochondria membrane potential*

To further support the previous finding, we measured the mitochondria membrane potential when mitoK and mitoSUR were concomitant co-expressed. The mitochondrion-selective tetramethylrhodamine dye (TMRM) was used to measure the mitochondrial membrane potential in Hela cells after the overexpression of mitoK and mitoSUR.

As shown in figure 6.3, overexpression of mitoK alone causes a significant decrease in mitochondrial membrane potential. Conversely, the overexpression of mitoSUR subunit alone does not affect organelle functions. The concomitant overexpression of the two subunits rescue mitochondrial membrane potential, supporting what we observed with calcium experiments.

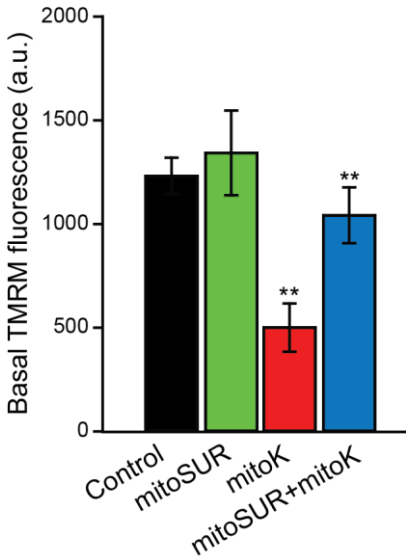

Fig.6.3. *MitoSUR inhibits mitoK channel activity*. *Hela cells were transfected with the indicated constructs. 36h after transfection, cells were loaded with tetramethylrhodamine methy (TMRM) ester and fluorescence was measured as described in Material and Methods section (n=6).*

- *6.4 MitoSUR guarantees ATP inhibition*

As described above, mitoSUR belongs to the ABC superfamily. Mitochondrial ABC proteins bind to adenine nucleotides through theirnnucleotide-binding domains (NBDs). These

domains contain the conserved Waker A (G-X-X-G-X-G-K-S/T) and Walker B motifs (ϕ-ϕ-ϕ-ϕ-D, where ϕ represents a hydrophobic residue), which mediate ATP binding.

In figure 6.4 we can observe the diagram of the structure of a representative ABC protein of the plasma membrane: the transmembrane domains form a pore throught the plasma membrane and associate with the nucleotide binding domains, which are found on the cytosolic face of the membrane. Stars indicate the ATP binding sites.

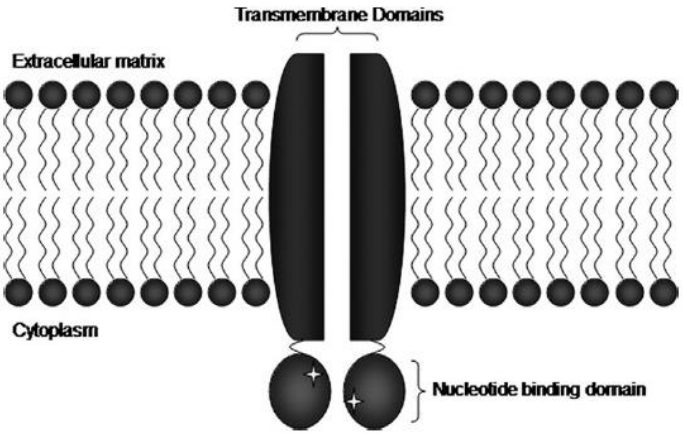

Fig. 6.4. Diagram of a typical ABC transporter protein.

In order to confirm the specificity of the gating by intracellular nucleotides, we generated a mitoSUR mutant (mitoSUR^{K513A}) unable to bind ATP through site directed mutagenesis of the Walker motif, as shown in figure.

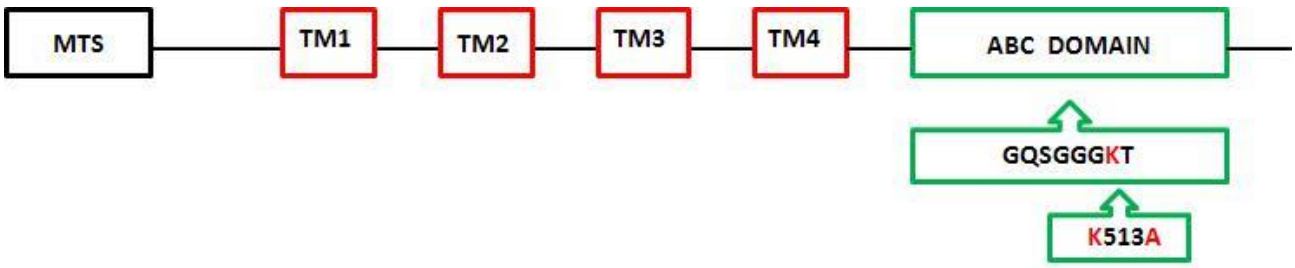

We tested the mutant form of mitoSUR both in mitochondrial calcium and mitochondria membrane potential in the concomitant overexpression of mitoK.

As shown in figure 6.4A-B, overexpression of mitoK alone causes a significant decrease of mitochondrial calcium uptake after histamine stimulation. Conversely, the overexpression of the mitoSUR^{K513A} subunit alone does not affect organelle functions, similarly to the overexpression of the wild type form of mitoSUR. Most importantly, the concomitant

overexpression of mitoK and mitoSUR^{K513A} subunit is not able to rescue the loss of mitochondrial calcium uptake caused by mitoK overexpression, thus enforcing the notion that ATP acts as channel inhibitor.

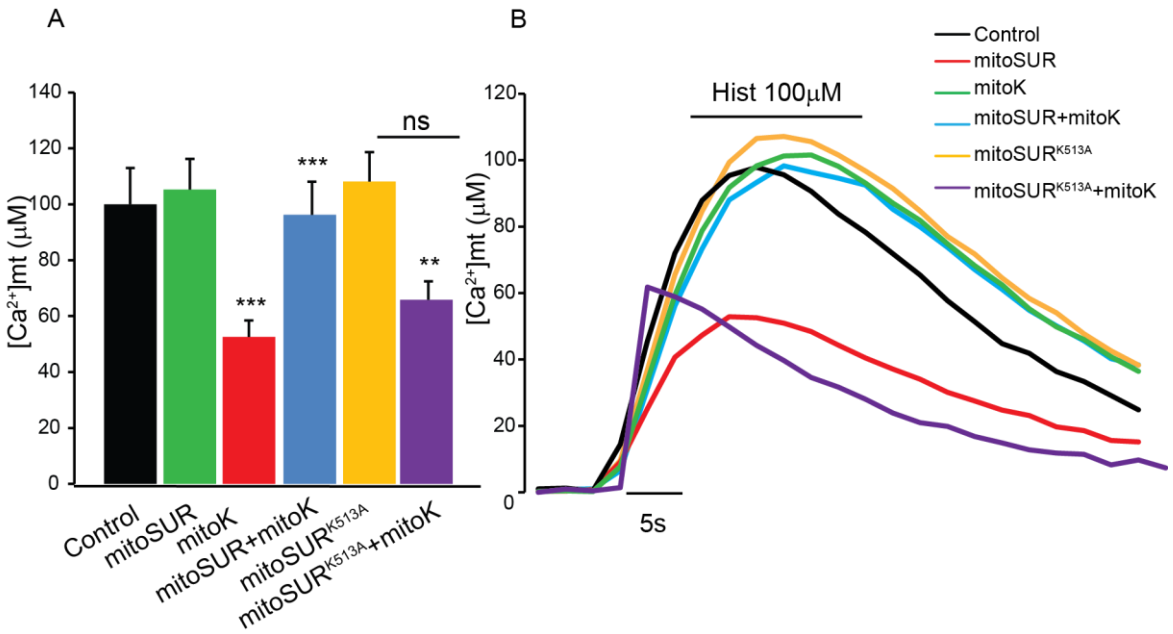

Fig.6.4.A-B. ***MitoSUR guarantees ATP inhibition.*** *(A-B) Hela cells were transfected with the indicated constructs together with mitochondrial-targeted aequorin probe and agonist induced peaks of matrix [Ca^{2+}] was measured (n=6, ***p < 0.001).*

Similar results have been obtained for the measurement of the mitochondrial membrane potential. As shown in figure 6.4C, mitoSUR^{K513A} is not able to rescue the loss of mitochondrial membrane potential caused by mitoK overexpression.

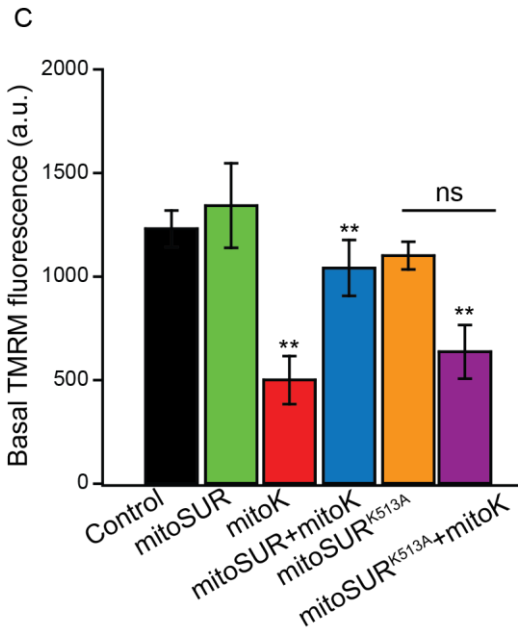

Fig. 6.4C. ***MitoSUR guarantees ATP inhibition.*** *Hela cells were transfected with the indicated constructs. 36h after transfection, cells were loaded with tetramethylrhodamine (TMRM) methyl ester and fluorescence was measured as described in Material and Methods section (n=6).*

- *6.5 Effects of co-expression of mitoK and mitoSUR in a planar lipid bilayer*

The data presented so far strongly support the notion that mitoK and mitoSUR form the long-sought mitoK$_{ATP}$. However, the unambiguous demonstration of their genuine channel activity and pharmacological profile necessarily relies on *in vitro* reconstitution approaches. We thus expressed both mitoK and mitoSUR in a cell-free transcription/translation system based on wheat germ lysate, where membrane contaminants are absent. We then purified the recombinant proteins and reconstituted them in planar lipid bilayers.

As shown in figure 6.5A-B, mitoK and mitoSUR together form a channel i) selective for monovalent cations, ii) sensitive to ATP, iii) activated by diazoxide, a well-known pharmacological activator of the mitoK$_{ATP}$. Overall, all these features recapitulate the fundamental traits of the mitoK$_{ATP}$.

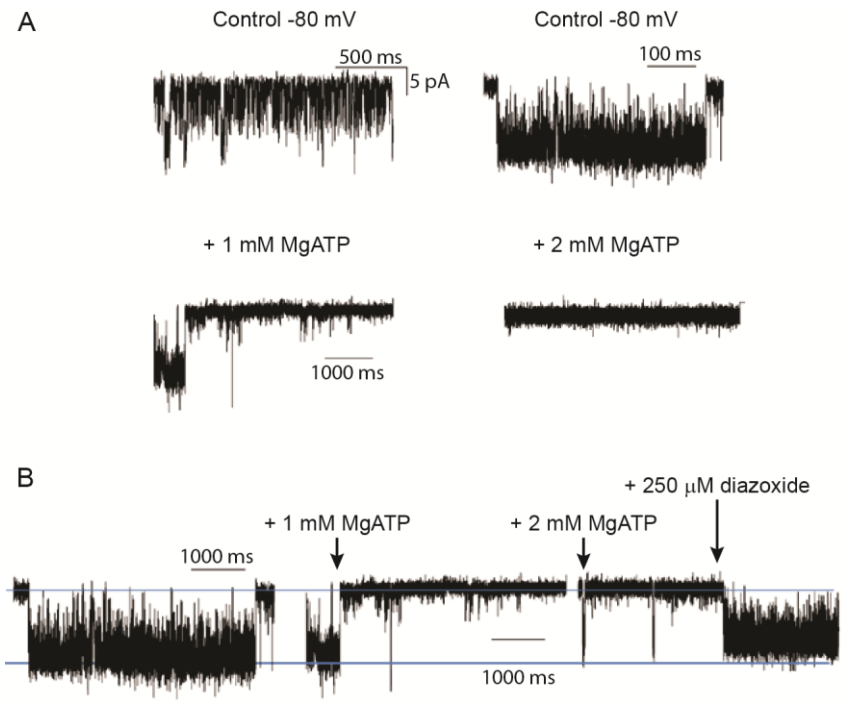

Fig.6.5A-B. ***MitoK and mitoSUR form a functional mitoK$_{ATP}$ in vitro****. Recombinant mitoK and mitoSUR were purified, reconstituted in a planar lipid bilayers and electrophysiological recordings were performed in 150mM KCl by adding the indicated compounds.*

7. Physiological role of the mitoK$_{ATP}$

One of the key questions regarding the mitoK$_{ATP}$ is how its activity impacts on organelle function. Although a number of hypothesis has been proposed and tested, significant discrepancies are present in the literature on the field. Most importantly, these experimental data rely uniquely on pharmacological approaches that lack selectivity. The discovery of the molecular identity of the mitoK$_{ATP}$ finally allows testing its impact on mitochondrial functions by using genetic procedures.

In order to investigate this aspect, we generate Hela cells knockout for mitoK by using the Crispr/Cas9 technology. Crispr (clustered regularly interspaced short palindromic repeats) are DNA loci containing short repetitions of base sequences. When paired with Cas9 nuclease, Crispr can cleave genomic DNA in a site-specific manner, thus knocking out gene expression. Guide RNAs (gRNA) are designed to a specific genomic sequence thus directing Cas9 to knockout the gene. The gRNA is a short synthetic RNA composed of a “scaffold” sequence necessary for Cas-9 binding and a user-defined ~20 nucleotides “spacer” or

"targeting" sequence which defines the genomic target to be modified. In our case, two different guides targeting different gene regions are designed and together with Cas9 are cloned into lentiviral vectors, packaged into viral particles and transduced into target cells. The genomic target can be any ~20 nucleotide DNA sequence, provided it meets two conditions: i) the sequence is unique in the host genome, ii) the target is present immediately upstream of a Protospacer Adjacent Motif (PAM). The PAM sequence is absolutely necessary for target binding and the exact sequence is dependent upon the species of Cas9. In figure 7A, is reported the designed strategies for mitoK gene knockout.

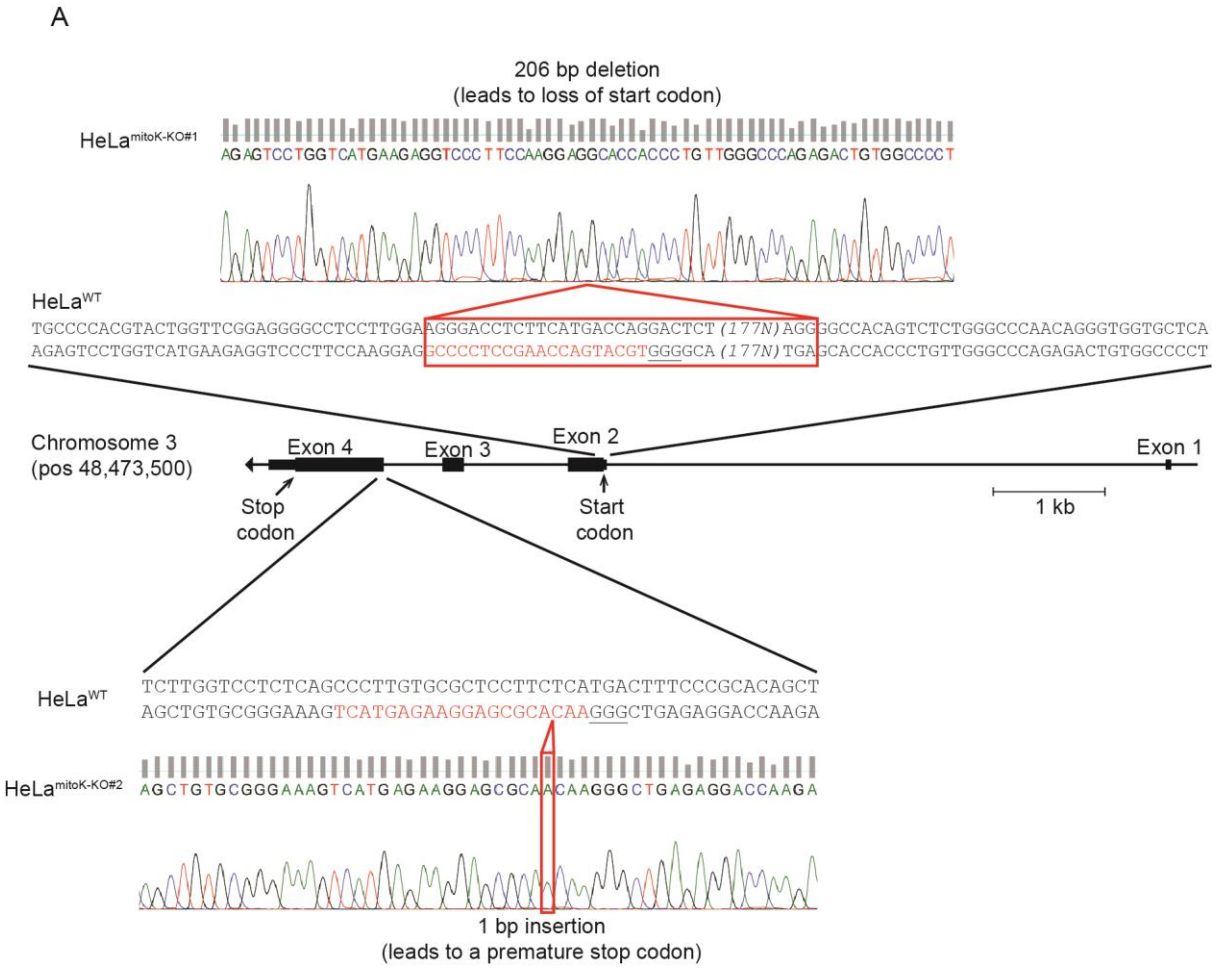

Fig.7A. ***Designed strategies for mitoK gene knockout****. Overall organization of mitoK gene and insets containing the Crispr guide sequences (colored in red, PAM sequence is underlined); the genomic sequences of the resulting Hela mitoK^{-KO} clones are shown as chromatograms.*

Several clones were grown and the efficient gene ablation was tested at protein level through Western blot. As shown in figure 7B, the resulting clones completely lack the mitoK protein.

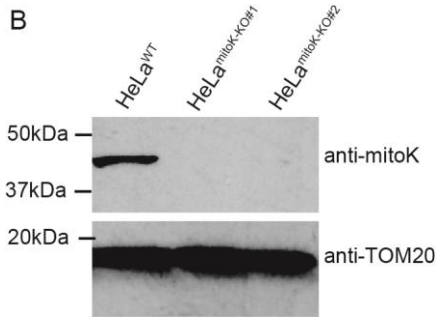

Fig.7B. ***Validation of mitoK-Knockout cells****. Western blot of the selected clones probed with the indicated antibodies.*

- *7.1 MitoK^{KO} cells show a peculiar ultrastructure*

In order to dissect the phenotype of Hela mitoK^{KO} cells, we performed transmission electron microscopy. Hela cells (as control), cells overexpressing mitoK and mitoK^{KO} cells were plate in a 24 wells and fixed for electron microscopy after 36 hours.

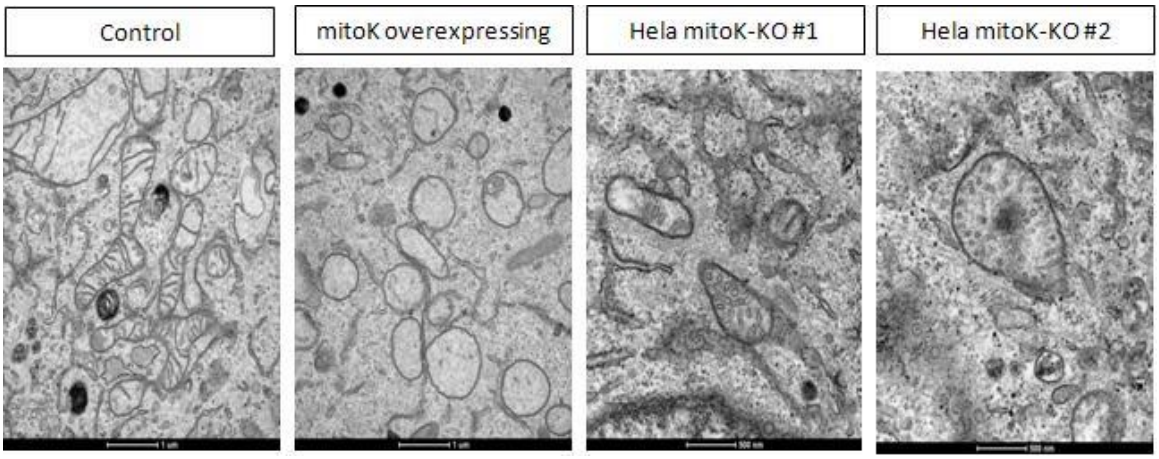

Fig.7.1. ***MitoK-Knockout cells show a peculiare ultrastructure****. Representative electron microscopy images of mitochondrial ultrasutructures in control, overexpressed mitoK and mitoK-Knockout Hela cells*.

As shown in figure7.1, mitochondria from control cells appeared as tubular structures with well-defined and tight cristae; mitochondria that overexpressed mitoK became dot-like structures and lost their tubular aspect (as reported in figure 7.1); most importantly, ablation of mitoK leads an impairment of mitochondrial ultrastructure with numerous abnormal and enlarged cristae.

- *7.2 MitoK^{-KO} cells show flickering of mitochondrial membrane potential*

In order to further investigate if the particular structure of the cristae that characterized mitoK^{-KO} cells could have an impact in other mitochondrial parameters, we measured the mitochondrial membrane potential with TMRM probe.

In these cells, mitochondrial membrane potential is overall intact, but we noticed that Hela mitoK^{-KO} cells undergo to asynchronous, rapid and transient depolarizations of single mitochondria, a phenomenon known as “flickering” or “flashes” of mitochondria membrane potential. Representative traces of this peculiar behavior can be found in fig. 7.2A, where the TMRM intensity of the highlighted individual organelles is tracked through time. We are also able to quantify the number of depolarization events every 5 minutes ($\Delta\psi_m$ flickering) (Fig.7.2B), and demonstrated that the loss of mitoK leads to a drastic increase of $\Delta\psi_m$ flickering frequency.

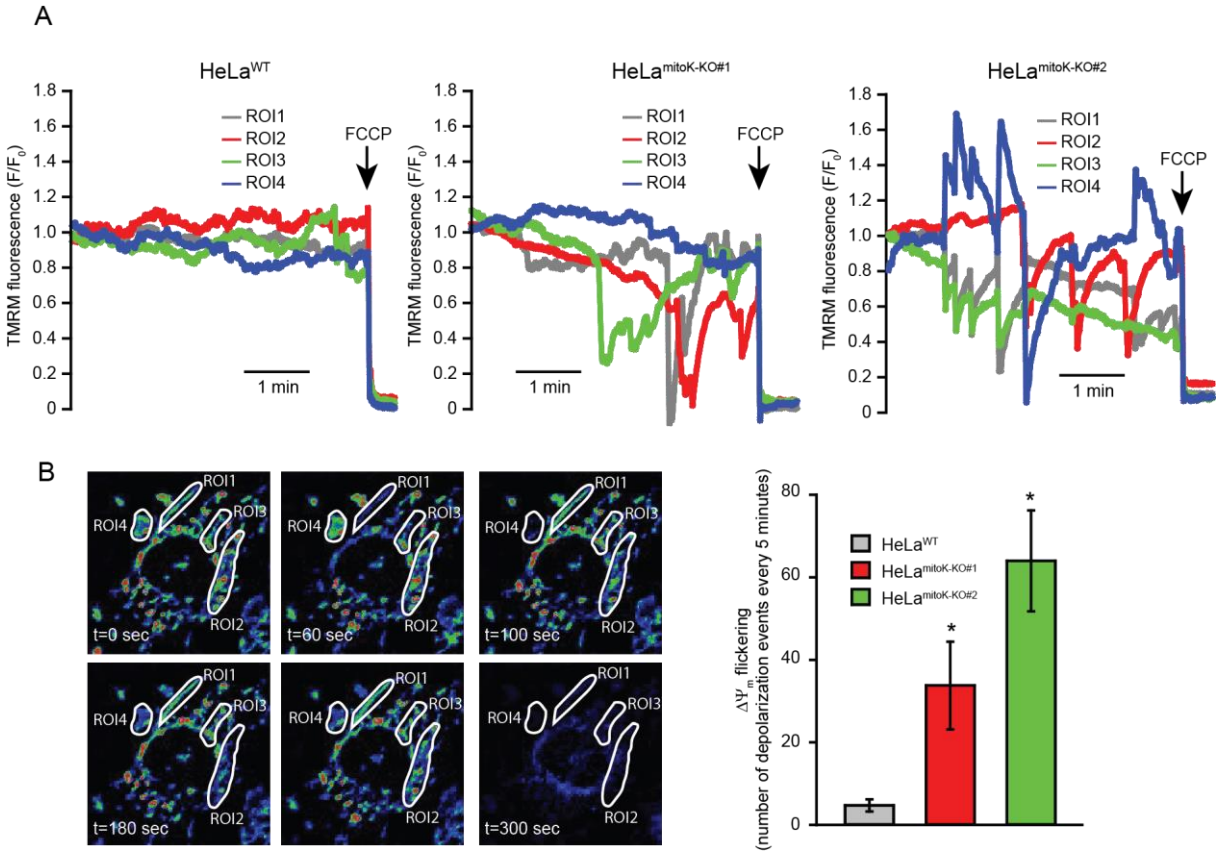

Fig.7.2A-B. ***Loss of mitoK triggers the flickering of mitochondrial membrane potential (ΔΨ)****. The indicated clones were loaded with TMRM and fluorescence was monitored for 5 minutes. (A) Representative traces show the normalized mean grey values of individual mitochondria trough time. (B) Representative TMRM images of one mitoK^{KO} cell line at the indicated time points and quantitative analysis of flickering events.*

➢ *7.3 MitoK^{-KO} cells show an impairment of oxygen consumption rate (OCR)*

In order to further evaluate the role of mitoK$_{ATP}$ in mitochondrial functions, we measured the oxygen consumption rate in control and mitoK-knockout Hela cells. This parameter was measured in intact cells by using of a Seahorse –XF Analyzer platform. Mitochondrial respiration was fist inhibited by addition of Oligomycyn (point A), then prompted by FCCP (point B) and finally dropped by Rotenone and Antymycin (point C and D).

Oxygen consumption rate (OCR) is greatly impaired in Hela mitoK^{-KO} cells when compared to their wild type counterparts, in both basal, leaky (i.e. olygomycin induced) and maximal (i.e. FCCP induced) respiration (Fig.7.3A).

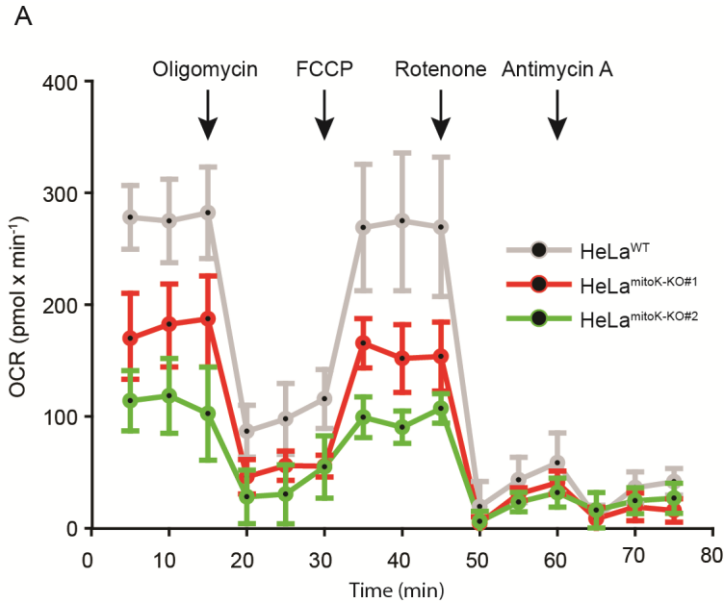

Fig.7.3A. ***Loss of mitoK impairs mitochondrial respiration.*** *Oxygen consumption rates of the indicated cell lines were measured through extracellular flux analyzer.*

In order to test if the impairment of mitochondrial respiration is due to a dysregulation of respiratory chain complexes, we analyzed the overall expression levels of ETC components through western blot analysis (Fig.7.3B). This revealed that the loss of mitoK causes no major defect in the expression levels of respiratory chain complexes compared to control Hela cells.

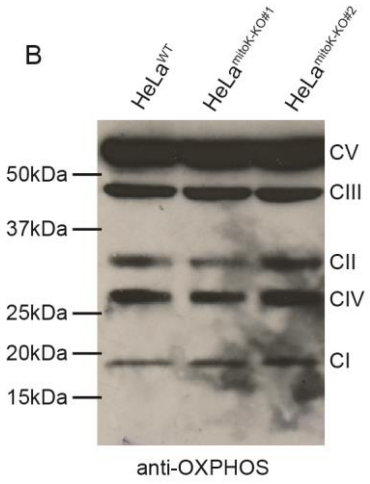

Fig.7.3B. ***Loss of mitoK does not affect protein levels of ETC complexes****. Proteins were extracted and blotted from the indicated cell lines and probed with the indicated antibody.*

DISCUSSION AND CONCLUSION

After decades of intense investigation, the molecular identity of the mitochondrial Ca^{2+} uniporter has been identified. This exciting result opened new developments in the clarification of the mechanisms of mitochondrial Ca^{2+} homeostasis, the regulation of cellular metabolism and cell survival. Of course, the discovery of MCU is only the beginning to understand the phenomenon of the accumulation of mitochondrial Ca^{2+}. Indeed there are a lot of conditions that can change the dynamics of the $[Ca^{2+}]$mt and consequently several modulators of this channel must exist. At the beginning, the aim of my PhD research was to identify a protein that could play the role of MCU interactor. We started from the same approach that was used for the identification of the Mitochondrial Calcium Uniporter. We screened *in silico* the MitoCarta database, with the following parameters: i) ubiquitous expression in mammalian tissue, ii) presence in those organisms in which mitochondrial Ca^{2+} transport with the properties of MCU was reported, iii) presence of coil-coiled domains and iv) absence in *S. cerevisiae*. This analysis allowed us to identify an interesting candidate, the protein coiled-coil domain containing 51 (CCDC51).

First, we confirmed the mRNA expression in multiple tissues through real-time PCR analysis, including, heart, kidney, liver, skeletal muscle and brain (Fig.2A). Overall, the expression profile was similar to that observed for the MCU in the same tissues (Fig.2B). This first data could therefore support our original hypothesis. Therefore, CCDC51 was cloned into plasmid vectors *pcDNA3.1* with Flag, V5 or GFP tags in order to perform a detailed characterization of its biochemical features and functions. Immunofluorescence demonstrated the mitochondrial localization of the protein (Fig 3.1A-B-C). In order to understand the correct localization at sub-mitochondrial level, we have combined different biochemical techniques, including: isolation of mitochondria and mitoplasts (i.e. mitochondria lacking the outer mitochondrial membrane), extraction of soluble proteins with Na_2CO_3 and proteinase K protection assays. Western Blot analysis of these fractions showed that CCDC51 is a mitochondrial protein located either in the IMM or in the matrix, because its specific band is progressively enriched in the mitochondria and mitoplast fraction (and absent in the OMM or IMS) when compared with the total homogenate (Fig.3.1D). The assay with Na_2CO_3 allows

us to discriminate between soluble and membrane proteins. According to our data, CCDC51 is a membrane protein, since it is present exclusively in the pellet fraction (Fig.3.1E). By combining these data, we concluded that CCDC51 is a protein of inner mitochondrial membrane. Finally, we performed a classical proteinase protection assay in order to understand the topology of the protein. Taking into account the presence of two predicted transmembrane domains, our data indicate that CCDC51 is located in the inner mitochondrial membrane with its NH_2 terminal part and its COOH terminal parts exposed to the matrix (Fig.3.1F-G).

These methods are able to characterize the protein from a structural point of view. However, our main aim is to understand the possible functions that the protein exerts at the level of mitochondria and its possible interaction with the MCU. First of all, to better understand the implication of CCDC51 in calcium homeostasis, we have studied the Ca^{2+} dynamics using aequorin-based probes in HeLa cells. We observed a strong decrease of agonists-induced mitochondrial Ca^{2+} transients (Fig.4.1C-D). This effect is not dependent on a deregulation of Ca^{2+} homeostasis in the other compartments. As an example, in the cytosol there are no differences between control and CCDC51-overexpressing cells (Fig.4.1A-B). Once identified the specific effect of CCDC51 at the level of mitochondria, we tested the hypothesis of a possible interaction with the uniporter. We studied the effects of a co-expression of both proteins (MCU and CCDC51) on mitochondrial Ca^{2+} dynamics in Hela cells. In this experimental setup, CCDC51 can decrease mitochondrial Ca^{2+} accumulation even when MCU is overexpressed (Fig.4.2A-B). This indicates that the effect of CCDC51 is independent of the amount of the MCU in the cells, thus suggesting that CCDC51 may not be an MCU modulator. This information was further confirmed in the analysis of the interaction between MCU and CCDC51 through FRET analysis. The co-expression of both chimeras (MCU-GFP and CCDC51-mCherry) reveals no significant interaction between the two proteins (Fig.4.3A-B). Overall, we can exclude a direct effect of CCDC51 on the mitochondrial Ca^{2+} uptake machinery.

We thus decided to investigate other mitochondrial parameters that may justify a reduction in Ca^{2+} accumulation. The impairment of mitochondrial Ca^{2+} uptake can be indeed secondary to changes in the driving force for Ca^{2+} accumulation (i.e. collapse of mitochondrial membrane potential, $\Delta\Psi$), organelle shapes, ER-mitochondria contact sites. First of all, we

analyzed the effects of CCDC51 overexpression on mitochondrial morphology. The images acquired through laser scanning confocal microscopy show that the protein induces a clear mitochondrial fragmentation (Fig4.6A). We hypothesized that CCDC51 could be directly implicate in the mechanism of mitochondrial fission. Indeed, it is known that the proteins involved in this process produce mitochondrial fragmentation when overexpressed. To test this aspect, we analyzed confocal images of Hela cells that overexpressed CCDC51 in combination with DRP1 (Dynamin-related protein 1) -protein implicated in mitochondrial fission- and DRP1-K38A, the dominant negative form of DRP1 that prevents the formation of fragmented mitochondria. Confocal images suggest us to rule out a possible involvement of CCDC51 in the mecchanism of mitochondrial fission. Indeed, mitochondria that overxpress CCDC51 and DRP1-K38A are fragmentated, underline that the inihibition of fission (throught DRP1-K38A) is not sufficent to restore the phenotype that characterizes overexpression of CCDC51 (Fig.4.6B). Once excluded an implication in the regulation of mitochondrial morphology, we analyzed the effects of CCDC51 overexpression on cristae structure through electron microscopy and we observed that an overexpression of this protein induces a total collapse of cristae (Fig.4.5A). This aspect is in agreement with the secondary effects that we observed when CCDC51 is overexpressed in Hela cells. Indeed we measured the mitochondrial membrane potential using fluorescent indicator TMRM. The results have clearly shown that mitochondria that overexpressed CCDC51 are almost devoid of potential (Fig.4.4). Then, we hypothesized that this dysregulation could be due to a premature opening of the PTP. To test the possible involvement of the PTP has been used the most effective inhibitor, cyclosporine A (CsA). The experiment performed was to grow Hela cells in the presence of cyclosporine. The expected result is to appreciate a slight increase in [Ca^{2+}] in control cells, and a decrease in [Ca^{2+}] for cells that overexpressed CCDC51 like the same cells transfected with the protein but not treated with cyclosporine A (Fig.4.5B-C). However, our results didn't validate our hypothesis. Even in the presence of cyclosporine, cells overexpressing CCDC51 showed the same decrease in mitochondrial calcium accumulation, indicating that the loss of mitochondrial membrane potential is not due to PTP opening. This data, together with the results on mitochondrial calcium accumulation and mitochondrial membrane potential, remarked that CCDC51 and MCU have an independent effect.

Overall, we demonstrated that CCDC51 overexpression leads to a major dysregulation of multiple mitochondrial parameters, including organelle fragmentation and swelling, loss of membrane potential and decrease of mitochondrial Ca^{2+} accomulation. All these effects are in line with an increase of cation permeability of the inner mitochondrial membrane and they are indeed mimicked by treatment with mitochondrial uncouplers, including valinomycin, a potassium ionophore. Taken together all these results, we thus hypotized that CCDC51 could be act as an ion channel. The only way to unambigously test this hypothesis is to investigate the function of the purified protein in an heterologous system. In order to get this fundamental piece of data, we first expressed the recombinant CCDC51 protein in a wheat-germ cell-free transcription/translation system, and then inserted the purified protein into lipid bilayers. We then tested its electrophysiological activity in a medium containing 150mM KCl. We could demonstrated that CCDC51 is sufficient to form a functional channel. Importantly its activity was completely abolished by the addition of tetraethylammonium chloride, a general inhibitor of potassium channels. Thus CCDC51 alone acts as potassium channel (Fig.5A-B). There are several potassium channel reported to be present at the level of the inner mitochondrial membrane (see Introduction). However, most of them (mitoBK$_{Ca}$, two-pore doomain TASK-3 and mitoK$_v$1.3) already have a clear molecular composition, with the notable exception of the mitochondrial ATP-sensitive K^+ chennel (mitoK$_{ATP}$). We thus wondered wether CCDC51 could be the mitoK$_{ATP}$.

ATP-sensitive potassium channels (KATP) are K^+-selective channels gated by intracellular nucleotides. They are primarily located at the plasma membrane (pmKATP), but several evidences indicate they are also present in intracellular membranes, in particular in the inner mitochondrial membrane (mitoK$_{ATP}$). The mitocondrial ATP-sensitive potassium channels is one of the most controversial topics in the field of mitochondrial reserch, since even its very existence is a matter of debate (Garlid KD, Halestrap AP., 2012). MitoK$_{ATP}$ mediates the electrophoretic transport of potassium ions inside the organelle matrix, thanks to the large driving force represented by the mitochondrial membrane potential, and its inhibited by normal physiological ATP concentrations. The main features of the mitoK$_{ATP}$ were originally described 1991 through direct patch clamp of mitoplasts (Inoue I et al, 1991). Since then, the mitoK$_{ATP}$ was well described from the pharmacological point of view and both channel openers (i.e diazoxide) and inhibitors (i.e sulphonylureas and 5-hydroxydecanote) have been

found (Szewczyk et al.,2002). Drugs targeting K_{ATP} channels are widely recogized to be useful in the treatment of several pathologies (Edwards G, Weston AH., 1993). Importantly, some of their therapeutic uses are due to the modulation of ATP-sensitive channels of the plasma membrane (pmK_{ATP}), but others largely depend on their effects on $mitoK_{ATP}$. Indeed, diazoxide efficiently protects the heart from ischemia reperfusion injury (Garlid K.D. et al., 1997), even in the absence of cardiac pmK_{ATP} (Sato T. et al., 2000). However, despite the significant efforts that have been spent in this direction, the molecular identity of this channel remained elusive.

Unfortunately, our data show that CCDC51 *per se* fails to show any ATP sensitivity. However, we reasoned that the ATP sensitivity could be conferred by a regulatory channel subunit, similary to what happens in pmK_{ATP}. Indeed, pmK_{ATP} channels are heterooligomers composed by a tetramer of Kir (K^+-selective inward rectifier, i.e the channel forming subunit) associated with four regulatory sulfonylurea receptor (SUR) subunits (belonging to the ABC superfamily), all arranged in an octomeric complex. SURs do not act as "pumps", and their function is essential to regulate K_{ATP} channels activity. Starting from this hypothesis, we looked to mitochondrial proteins of the ABC family. Among these, we found one particular promising candidate to act as putative SUR subunit. Indeed, the protein encoded by the ABCB8 gene share the same tissue expression of CCDC51. In addition, it has already been described to be involved in $mitoK_{ATP}$ (Ardehali et al., 2005) and mitochondria derived from ABCB8-null mice display an overall ultrastructure resembling CCDC51-overespressing mitochondria. Our working hypothesis is that $mitoK_{ATP}$ has the same overall molecular organization of K_{ATP} of plasma membrane: CCDC51 acts as K-permeant subunit (and will be thus named as mitoK hereafter), while ABCB8 acts as SUR subunits (and will be thus named as mitoSUR hereafter). According to this view, the concomitant overexpression of mitoK and mitoSUR should restore the mitochondrial dysfunction caused by the overexpression of mitoK alone, since the mitoSUR subunit confers the correct gating and closes the channel in normal physiological conditions. To confirm this hypothesis, we first check whether mitoK and mitoSUR interact each other. Co-immunoprecipitation experiment shown in figure 6.1 demonstrate the physical interaction between these two proteins. Then, we measured both mitochondrial membrane potential and organelle calcium transients. As shown in figure 6.2A-B and in figure 6.3, overexpression of mitoK alone causes a significant decrease of both

these parameters. Conversely, the overexpression of the mitoSUR subunit alone does not affect organelle functions. Most importantly, the concomitant overexpression of the two subunits perfectly rescue mitochondrial membrane potential and Ca^{2+} dynamics, suggesting the restoration of the proper physiological channel gating. Overall, the data presented so far strongly support the notion that mitoK and mitoSUR form the long-sought mitoK$_{ATP}$. However, the best way to demonstrate that mitoK and mitoSUR form a functional channel is *in vitro* reconstitution approach. We thus tested the co-expression of mitoK and mitoSUR in a cell-free transcriptional/translation system based on wheat germ lysate. We then purified the recombinant proteins and reconstituted them in planar lipid bilayers. Strikingly, mitoK and mitoSUR together form a channel i) selective for monovalent cations, ii) blocked by tetraethylammonium chloride (TEA), iii) sensitive to ATP (Fig.6.5A), iv) activated by diazoxide (Fig.6.5B). Overall, all these features recapitulate the fundamental profile of the mitoK$_{ATP}$.

In order to confirm that ABCB8 is the mitoSUR subunit that can regulate the activity of mitoK through ATP binding, we generated a mitoSUR mutant (mitoSUR^{K513A}) unable to bind ATP through site direct mutagenesis of the Walker motif. This mutant is not able to rescue the loss of mitochondrial calcium accumulation and mitochondrial membrane potential caused by mitoK overexpression (Fig.6.4A-B-C), thus enforcing the notion that ATP act as channel inhibitor.

Much of the debate on the mitoK$_{ATP}$ is focused on its physiological role. According to the available literature, mitoK$_{ATP}$ channels are believed to be protective in ischemia-reperfusion injury. However, the broad conservation profile among all vertebrates suggests that the mitoK$_{ATP}$ should also have a primary housekeeping function. In order to analyze this aspect, we generated Hela cells knockout for mitoK by using the Crispr/Cas9 technology. Two different guides targeting different gene regions were designed (Fig.7A) and several Hela mito$^{K\text{-}KO}$ clones were obtained (Fig.7B). Overall, ablation of mitoK leads to no gross defects in mitochondrial morphology, although an impairment of cristae structure become evident through electron microscopy (Fig.7.1). Mitochondrial membrane potential is overall intact, but we noticed that Hela mitoK^{-KO} cells undergo to asynchronous, rapid and transient depolarizations of single mitochondria, a phenomenon known as “flickering” of mitochondrial membrane potential. Representative traces of this peculiar behavior can be found in figure 7.2A-B, where TMRM intensity of the highlighted individual organelles is

tracked through time. Although expression of respiratory chain complex is unaffected (Fig.7.3B), oxygen consumption rate (OCR) is greatly impaired in Hela mitoK^{-KO} cells when compared to their wild type counterparts, in both basal and maximal (i.e FCCP induced) respiration (Fig.7.3A). As already reported, mitochondrial K^+ homeostasis is fundamental to regulate mitochondrial matrix volume: while excessive accumulation leads to organelle swelling, a decrease in K^+ uptake is predicted to cause matrix contraction (Garlid K.D., Paucek P., 2003), with obvious expected consequences on the performance of the oxidative phosphorylation.

Overall, our data indicates that mitoK$_{ATP}$ is a central regulator of mitochondrial function that modulates the efficiency of energy production according to the ATP availability through the regulation of matrix volume. Based on strong and robust preliminary data, we have now identified the key molecular components of the mitoK$_{ATP.}$ This important discovery allows the investigation of the structure, the function and the pathophysiological role of the mitoK$_{ATP}$ channels. This research proposal will revitalize a poorly explored topic in organelle biology and will provide novel molecular targets with potential high therapeutic impact.

MATERIAL AND METHODOS

Bioinformatic screening

The MitoCarta database was screened for ubiquitously expressed proteins and proteins containing one or more transmembrane domains predicted using the TMHMM algorithm and at least one predicted coiled-coil domain predicted using PCOILS. Sequences of these candidates were retrieved and aligned with the *Saccharomyces cerevisiae* proteome by a standard Gonnet matrix to exclude homologues. All alignments with a P-value <0.001 were excluded. Out of 1158 proteins present in MitoCarta, only 10 fulfilled these requirements.

Cell culture, transfection and proteomic analysis

All the experiments were performed in HeLa cells cultured in Dulbecco's modified Eagle's medium (DMEM) (Lifetechnologies), supplemented with 10% Fetal bovine serum (FBS) (Lifetechnologies), containing penicillin (100 U/ml) and streptomycin (100µg/ml). For some experiments we used also Hek293A cultured in the same conditions of Hela cells.
Cells were cultured in Galaxy-S incubator at 37°C and 5% CO_2.
Cells were transfected with a standard Ca^{2+}-phosphate procedure. For Ca^{2+}-phosphate transfection procedure the following stock solution need to be prepared and conserved at -20°C until used:
- $CaCl_2$ 2.5 M.
- HEPES Buffered Solution 2X (HBS): 280 mM NaCl, 50 mM Hepes, 1.5 mM Na_2HPO_4, pH 7.12.
All solutions were sterilized by filtration using 0.22 µm filters. Just before the transfection procedure, cells are washed with fresh medium. For one 13 mm coverslip, 5 µl of 2.5 M $CaCl_2$ were added to the DNA dissolved in 45 µl of H_2O. Routinely, 4 µg of DNA were used to transfect 1 coverslip. The solution was then mixed under vortex with 50 µl of HBS and incubated for 20 to 30 minutes at room temperature. For one 24 mm coverslip the amount of solution and DNA were doubled while for 10cm dishes was used 50 µl of 2.5M $CaCl_2$, 20µg of DNA in 450 µl of H_2O and 500 µl of HBS. The transfection mix was then added directly to the cell monolayer. Sixteen hours after addition or the DNA, cells were washed with PBS

(two or three times until the excess precipitate is completely removed). Experiments were carried out 24-36 hours after transfection.

Western blotting and Antibodies

To monitor endogenous and overexpressed protein regulation, cells were lysate in RIPA-buffer (150 mM NaCl, 50 mM Tris, 1 mM EGTA, 1% Triton X-100, 0.1% SDS) and after 30' of incubation on ice, 40 µg of total proteins were loaded, according to BCA quantification. Proteins were separated by SDS-PAGE electrophoresis, in commercial 4-12% acrylamide gels (Life technologies) and transferred into nitrocellulose membranes (Life technologies) by wet electrophoretic transfer. Blots were blocked 1 hour at RT with 5% non-fat dry milk (BioRad) in TBS (0.5M Trizma –Sigma, 1.5M NaCl) solution (0.01% Tween) and incubated over night at 4°C with primary antibodies. Secondary antibodies were incubated 1 hour at RT. Washes after antibody incubations were done on an orbital shaker, three times for 10'each, with TBS-0,01% tween.

We used the following antibodies: anti-$CCDC51_{c\text{-}term}$ (1:10000, Sigma), anti-$CCDC51_{N\text{-}term}$(1:1000, Sigma) ,anti-GRP75 (1:1000, Santa Cruz), anti-HSP60 (1:5000, Santa Cruz), anti-β-tubulin (1:7500, Santa Cruz), anti-Flag (1:1000, Cell Signaling).

Secondary, HRP-conjugated antibodies (1:5000) were purchased from BioRad.

Co-immunoprecipitation

For the interaction between mitoSUR-Flag and mitoK, Hela cells were transfected with a calcium-phosphate procedure. After 48 hours of expression cells were lysate in an appropriate volume of lysis buffer (150mM NaCl, 1% Digitonin, 50mM Tris-HCl pH7.4, 1mM EGTA-Tris pH 7.4 and Complete EDTA-free protease inhibitor mixture (Roche Applied Science). Lysates were centrifuged at 13.000 r.p.m. for 10 min, and supernatant was transferred into new tubes. 1mg of proteins from the different conditions was incubated with Control Agarose Resina (Thermo) for 30 min at 4°C. This passage is called pre-clearing and reduce nonspecific binding of proteins to agarose beads. The precleared eluates were then centrifuged at 13.000r.p.m. for 10 min and the supernatant was incubated with monoclonal α-Flag-Agarose antibody (Sigma) for 3 hours at 4°C. When the lysate-beads

incubation time is over the tubes were centrifuged, the supernatants were removed from the beads and discard. The beads were washed with lysis buffer three times for 10 min in order to remove nonspecific binding. Then 50 µl of loading buffer 2X was added to the beads and the elution samples were boiled for 5 min at 95°C. The co-immunoprecipitation samples were analyzed by SDS-PAGE gel electrophoresis, transferred to Hybond-C Extra membrane (Amersham) and stained with Ponceau S solution. MitoSUR was visualized with polyclonal α-Flag antibody (Cell Signaling) and mitoK with polyclonal α-CCDC51 antibody (Sigma).

Aequorin as a Ca^{2+} indicator

Aequorin is a 21 kDa photoprotein isolated from jellyfish *Aequorea Victoria* which emits blue light in the presence of Ca^{2+}. The aequorin originally purified from the jellyfish is a mixture of different isoforms called "heterogeneous aequorin" (Shimomura, 1986). In its active form the photoprotein includes an apoprotein and a covalently bound prosthetic group, called coelenterazine. The apoprotein contains four helix-loop-helix "EF-hand" domains, three of which are Ca^{2+}-binding sites. These domains confer to the protein a particular globular structure forming the hydrophobic core cavity that accommodates the ligand coelenterazine. When Ca^{2+} ions bind to the three high affinity EF-hand sites, coelenterazine is oxidized to coelenteramide, with a concomitant release of CO_2 and emission of light (Head et al. 2000). Although this reaction is irreversible, an active aequorin can be obtained *in vitro* by incubating the apoprotein with coelenterazine in the presence of oxygen and 2-mercaptoethanol. Reconstitution of an active aequorin (expressed recombinantly) can be obtained also in living cells by simple addition of coelenterazine into the medium. Coelenterazine is highly hydrophobic and has been shown to permeate cell membranes of various cell types. Different coelenterazine analogues have been synthetized and are now commercially available.

The possibility of using aequorin as Ca^{2+} indicator is based on the existence of a well-characterized relationship between the rate of photon emission and the free $[Ca^{2+}]$. The first method used to correlate the amount of photons emitted to the free $[Ca^{2+}]$ was that described by Allen and Blinks (Blinks, 1978). In the following years, this system was improved to achieve a simple algorithm that converts luminescence into $[Ca^{2+}]$ values. Under physiological conditions of pH, temperature and ionic strength, this relationship is more than

quadratic in the range of [Ca^{2+}] 10-5-10-7 M. The presence of 3 Ca^{2+} binding sites in aequorin is responsible for the steep relationship between photon emission rate and free [Ca^{2+}]. The [Ca^{2+}] can be calculated from the formula L/Lmax where L is the rate of photon emission at any instant during the experiment and Lmax is the maximal rate of photon emission at saturating [Ca^{2+}]. The rate of aequorin luminescence is independent of [Ca2+] at very high (>10-4 M) and very low [Ca^{2+}] (< 10-7 M). However, as described below in more details, it is possible to expand the range of [Ca^{2+}] that can be monitored with aequorin.

Although aequorin luminescence is not influenced either by K^+ or Mg^{2+} (which are the most abundant cations in the intracellular environment and thus the most likely source of interference under physiological settings) both ions are competitive inhibitors of Ca^{2+} activated luminescence.

pH was also shown to affect aequorin luminescence but at values below 7. Due to the characteristics described above, experiments with aequorin need to be done in well-controlled conditions of pH and ionic concentrations, notably of Mg^{2+}.

Recombinant aequorins

Aequorin began to be widely used when the cDNA encoding the photoprotein was cloned, thus avoiding the purification of the native polypeptide and its microinjection. Moreover, the cloning of aequorin gene opened the way to recombinant expression and thus has largely expanded the applications of this tool for investigating Ca^{2+} handling in living cells. In particular, recombinant aequorin can be expressed not only in the cytoplasm, but also in specific intracellular compartments by including specific targeting sequences in the engineered cDNAs (Hartl et al., 1989). Extensive manipulations of the N-terminal of aequorin have been shown not to alter the chemiluminescence properties of the photoprotein and its Ca^{2+} affinity. On the other hand, even marginal alterations of the C-terminal either abolish luminescence or drastically increase Ca^{2+} independent photon emission. For these reasons, all targeted aequorins synthesized in our laboratory include modifications of the photoprotein N-terminal. Three targeting strategies have been adopted:

1. Inclusion of a minimal targeting signal sequence to the photoprotein cDNA. This strategy was initially used to design the mitochondrial aequorin and was followed also to synthesize an aequorin localized in the nucleus and in the lumen of the Golgi apparatus.

2. Fusion of the cDNA encoding aequorin to that of a resident protein of the compartments of interest. This approach has been used to engineer aequorins localized in the sarcoplasmic reticulum (SR), in the nucleoplasm and cytoplasm (shuttling between the two compartments depending on the concentration of steroid hormones), on the cytoplasmic surface of the endoplasmic reticulum (ER) and Golgi and in the subplasmalemma cytoplasmic rim.
3. Addition to the aequorin cDNA of sequences that code for polypeptides that bind to endogenous proteins. This strategy was adopted to localize aequorin in the ER lumen.
The construct used in our experiments is the mutated isoform of mitochondrial targeted aequorin (Brini M., 2008): mtAEQmut. It was generated to measure the [Ca^{2+}] of the mitochondrial matrix of various cell types. This construct includes the targeting presequence of subunit VIII of human cytochrome c oxidase fused to the aequorin cDNA. To expand the range of Ca^{2+} sensitivity that can be monitored the photoprotein was also mutated (Asp119>Ala). This point mutation affects specifically the second EF hand motive of wild type aequorin. The affinity for Ca^{2+} of this mutated aequorin (mtAEQmut) is about 20 fold lower than that of the wild type.

Luminescence detection

The aequorin detection system is derived from that described by Cobbold and Lee (Cobbold and Bourne, 1984) and is based on the use of a low noise photomultiplier placed in close proximity (2-3 mm) with aequorin expressing cells. Cells are seeded on 13-mm coverslips and put into a perfusion chamber. The volume of the chamber is kept to a minimum (about 200 µl). Cells are continuously perfused via peristaltic pump with KRB saline solution, thermostated via a water bath at 37°C.
The photomultiplier (Hamamatsu H7301) is kept into a dark box. The output of the amplifier-discriminator is captured by C8855-01-photoncounting board in an IBM compatible microcomputer and stored for further analysis.

Experimental procedures for Ca^{2+} measurements

Cells were seeded onto 13 mm glass coverslips and allowed to grow to 50% confluence. The day before measuring, cells were transfected with mtAEQmut aequorin plasmid (as previously described) together with the indicated plasmid.

The following day, coverslips with cells were incubated with 5 µM coelenterazine for 2 hours in KRB saline supplemented with 1mM $CaCl_2$, and then transferred to the perfusion chamber. All aequorin measurements were carried out in KRB saline solution. Agonists and other drugs were added to the same solution. The agonist stimuli used for maximal stimulation were: 100 µM histamine or 100 µM ATP, depending on the cell type.

The experiments were terminated by lysing cells with 100 µM digitonin in a hypotonic Ca^{2+}-rich solution (10 mM $CaCl_2$ in H_2O), thus discharging the unbound aequorin pool. The light signal was collected and calibrated into free [Ca^{2+}] values by an algorithm based on the Ca^{2+} response curve of aequorin at physiological conditions of pH, [Mg^{2+}] and ionic strength, as previously described (Brini M., 2008).

Measurement of Mitochondrial Membrane Potential

The measurement of mitochondrial membrane potential is based on the distribution of the mitochondrion-selective lipofilic cation ”tetramethyl rhodamine methyl ester” dye (TMRM, Life Technologies). It is fluorescent and membrane permeable and its distribution into intracellular compartments is controlled by electrochemical gradients. Hence, at low concentrations, its accumulation into mitochondria is driven by mitochondrial membrane potential (almost -180mV). In order to promote the correct distribution of the probe, cells were loaded with the dye-solution at very low concentration (20nM). Changes in mitochondrial membrane potential cause a redistribution of the dye between mitochondria and cytoplasmic environment. Cells were loaded with TMRM stock solution (in KRB saline solution) for 20’ at 37°C. The probe was excited at 560 nm and the emission light was recorded in the 590-650 nm range.

Images were taken every 10 s with a fixed 200 ms exposure time. FCCP (carbonyl cyanide p-trifluoromethoxyphenylhydrazone, 10 µM), an uncoupler of oxidative phosphorylation, was added after 12 acquisitions to completely collapse the electrical gradient established by the respiratory chain (ΔΨ). Data are expressed as difference between the TMRM fluorescence before and after FCCP depolarization. Imaging was performed in a wide field epifluorescence microscope (Zeiss Axiovert 200), equipped with a PlanFluar 40X/1.3NA objective, high-speed monochromator (PTI) coupled to a 75 W xenon arc lamp and an EMCCD camera (Photometris Evolve 512 Delta).

Förster Resonance Energy Transfer (FRET)

Hela cells were grown on 24 mm coverslips and transfected with the indicated combination of GFP, CCDC51-GFP, MCU-GFP, mCherry, CCDC51-mCherry or MCU-mCherry encoding plasmids when 50% confluent. GFP and mCherry were excited at 488 and 543 nm and their signals were collected in the 495-535 and 598-670 nm range respectively. A specific region of the specimen was bleached with a 1.5W 592 nm laser (4 passes at 30% power). Donor and acceptor were collected before and after bleaching and FRET efficiency was calculated from the background subtracted images with the formula:

$$FRET=\left(\frac{Donor_{post} - Donor_{pre}}{Donor_{post}}\right) * 100$$

Where $Donor_{pre}$ and $Donor_{post}$ are the mean fluorescence intensities in the selected region before and after bleaching. As internal control, no significant FRET was observed outside the bleached region. No bleaching of the donor was observed with this experimental setting. Pinhole was set to 1 airy unit and pixel size was adjusted to 150nm. Representative images were generated using the AccPbFRET plugin (Roszik et al., 2008) for ImageJ. All images were taken on a LEICA TCS STED CW system equipped with a 100x/1.4 N.A. Plan Apochromat objective.

Morphological analysis

- *Immunofluorescence*

HeLa cells were grown on 24 mm coverslips and transfected with CCDC51-Flag, CCDC51-GFP, and/or mtRFP encoding plasmid. After 24/36 hours, cells were washed with PBS, fixed in 4% formaldehyde for 10 minutes and quenched with 50 mM NH_4Cl in PBS. Cells were permeabilized for 10 minutes with 0.1% Triton X-100 in PBS and blocked in PBS containing 2% BSA for 1 hour. Cells were then incubated with primary antibodies (anti-Flag or anti-CCDC51) for 3 hours at room temperature and washed 3 times with 0.1% Triton X-100 in PBS. The appropriate isotype matched AlexaFluor conjugated secondary antibodies

(Lifetechnologies) were used and coverslips were mounted with ProLong Gold Antifade reagent (Lifetechnologies). Confocal images were acquired on a Leica SP5-TCS-II-RS. For all images, pinhole was set to 1 airy unit, pixel size was about 100 nm and a Z-stack was acquired for the whole depth of the cell by sampling at 130 nm in the Z plane. 488 nm Ar-laser line was used to excite GFP and its signal collected in the 492-537 nm range, while RFP fluorescence was excited by the 543 nm HeNe laser and its emission was collected in the 555-700 nm range. For each image, PMT gain was slightly adjusted in order to maximize signal and avoid saturation. Quantification of the number and the volume of the mitochondria were performed from ImageJ program.

Oxygen Consumption Rate Experiments

Mitochondrial respiration was followed in a kinetic mode by measuring the oxygen consumption rate (OCR) of cell monolayers with XFe Extracellular Flux Analyzer (Seahorse Bioscience) at 37°C. Baseline oxygen consumption rate (OCR) was measured followed by injections sequentially with oligomycin (2µM) to measure the ATP linked OCR, oxidative phosphorylation uncoupler FCCP (0.6µM) to determine maximal respiration, and rotenone (1µM) and antimicyn (1µM) to determine the non-mitochondrial respiration. Every point in traces represents the average of 6 different wells.

RNA extraction, reverse transcription, and quantitative realtime PCR

For the expression analysis of CCDC51 in mouse tissue, adult male C57BL/6 mice (28-30g) were used. Skeletal muscle (tibialis anterior), heart, brain, spleen, lung, liver kidney and visceral fat were excised from three age-matched animals. Total RNA was purified using SV Total RNA Isolation kit (Promega) following manufacturer instructions. The RNA was quantified with an Eppendorf Bio photometer Plus. From 400 nmol of total RNA of each sample, complementary DNA was generated with a cDNA synthesis kit (SuperScript II, Invitrogen) and analyzed by real-time PCR using the SYBR green chemistry (Bio-Rad). The primers were designed and analyzed with Primer3 (Rozen and Skaletsky, 2000). Real-time PCR standard curves were constructed by using serial dilution of cDNAs of the analysed samples, using at least four dilution points and the efficiency of all primer sets was between

98 and 102%. The housekeeping genes *Pol2Rf* were used as an internal control for cDNA quantification and normalization of the amplified products.

Constructs

Mouse CCDC51 was amplified from mouse skeletal muscle cDNA library by PCR using the following primers.

For cloning into pEGFP-N1: fw,5'-CTCGAGATGACAGGGTGCAGCCCCGT-3'; rv, 5'-GGATCCCGACTGGTCTTGAACAGCATGT-3'. The PCR fragment was cloned into XhoI and BamHI sites in pEGFP-N1 (Clonotech).

For the cloning of CCDC51-Flag into pcDNA3.1: fw, 5'- AAGCTTATGACAGGGTGCAGCCCCGT-3'; rv, 5'-CTCGAGTTACTTATCGTCGTCATCCTTGTAATCACTGGTCTTGAACAGCATGT-3'. The PCR fragment was cloned into HindIII and XhoI in pcDNA3.1 (Invitrogen).

For the cloning of CCDC51-V5 into pcDNA3.1: fw, 5'- AAGCTTATGACAGGGTGCAGCCCCGT-3'; rv,5'CTCGAGTTACGTAGAATCGAGGAGACCGAGAGGGTTAGGGATAGGCTTACCACTGGTCTTGAACAGCATGT-3'. The PCR fragment was cloned into HindIII and XhoI in pcDNA3.1 (Invitrogen).

For the cloning of CCDC51 in pIVEX 1.3 WG: fw, 5'- CCATGGCAACAGGGTGCAGCCCCGTGTT-3'; rv, 5'- CTCGAGACTGGTCTTGAACAGCATGT-3'. The PCR fragment was cloned into NcoI and XhoI in pIVEX1.3 WG (Roche).

For ABCB8 construct we used the commercial one from Origene pmCV6-ABCB8 (RC224948).

For the cloning of ABCB8 in pIVEX 1.3 WG: fw, 5'-GCGATCGCCCATATGCTGGTGCATTTA-3'; rv, 5'- CTACCGAGTACTTTAAACCTTATC-3'. The PCR fragment was cloned into NheI anD BamHI in pIVEX1.3 WG (Roche).

The generation of the pmCV6-ABCB8^{K513A} mutant was performed by mutagenesis PCR using the wild type pmCV6-ABCB8 vector as template and the mutagenesis primer: 5'-GGCCAGTCTGGCGGAGGAGCGACCACCGTGGCTTCCCTG-3'.

All constructs were verified by Sanger sequencing.

Protein expression and purification

In vitro: mitoK and mitoSUR were cloned into pIVEX1.3 WG, as described above. In vitro expression was performed by using a RT100 Wheat Germ CECF Kit (Roche). After expression, the reaction mix was solubilized with 2% Triton X-100 for 90min at 30°C under shaking.

Gel electrophoresis: SDS-PAGE was performed using 6M urea and standard protocols. Each lane was loaded with 30 µl of eluted fractions and 1µl of the reaction mix.

Electrophysiology

Electrophysiological experiments were carried out as previously described (Szabò I. et al., 2011; Teardo E., et al 2010). A Warner Instruments (Hamden) electrophysiological planar bilayer apparatus was used. Bilayers of approximately 150-200 pF capacity were prepared using azolectin in decane containing 1% chloroform (Sigma) across a 250 µM hole in a polystyrene cuvette. Azolectin was partially purified by precipitation with col acetone from a chloroform solution. The inside of the cuvette constituted the trans compartment. The standard experimental medium was 150mM KCl. The lipid membrane was built under symmetric ionic conditions and both chambers contained 3ml of solution. The contents of both chambers were stirred by magnetic bars when desired. Connections to the electrodes were provided by agar bridges. Purified proteins were added to the cis side. Control experiments with empty membrane or with detergents used for the purification showed no activity. All voltages reported are those of the cis chamber, zero being assigned by convention to the trans (grounded) side. Currents are considered as positive when carried by cations flowing from the cis to the trans compartments. A BC-525C unit and headstage were used to control parameters and amplify signals. Output was recorded with a 10kHz bandwidth on videotape using a Medical System PCM-2 interface. Data were acquired at 2kHz, filtered at 500 Hz and analyzed offline using the pClamp program set (Axon Instruments). Conductance was determined by averaging the measured amplitudes of single channel events ($n \geq 50$) at various applied voltages.

Crispr/Cas9 technology

For generating mitoK^{-KO} cell lines, two Cas9 guides targeting different regions of the human CCDC51 gene were designed (GCCCCTCCGAACCAGTACGT and TCATGAGAAGGAGCGCACAA) and cloned into the BsmBI site of the LentiCrisprV2 plasmid, a kind gift of Feng Zhang (Addgene plasmid #52961). Lentiviral particles were produced by transfecting 293T cells with the transfer plasmids together with pRSV-Rev (Addgene #12253), pMDLg/pRRE (Addgene #12251) and pMD2.G (Addgene #12259) plasmids, kindly provided by Didier Trono. Three days after transfection, the supernatants were collected, centrifuged and cleared through 0.45μm cellulose acetate filters. Target cells were infected with viral particles and selected with puromycin for one week. Dilution cloning was performed to obtain different monoclonal cell populations that were screened and validated for CCDC51 gene ablation through Western blot.

Statistical analysis of data

Statistical data are presented as mean ± s.e.m, unless otherwise specified. Significance was calculated by Student's t-test.

BIBLIOGRAPHY

Ardehali H, Dong P, Machamer C, Marban E (2005) Removal of the mitochondrial targeting signal leads to targeting of mitochondrial membrane proteins to the secretory pathway. Biochem Biophys Res Commun 338:1143–1151.

Ardehali H, O'Rourke B, Marbán E (2005) Cardioprotective role of the mitochondrial ATP-binding cassette protein 1. Circ Res 97:740–742.

Ashcroft F.M., Gribble FM. (1999) ATP-sensitive K^+ channels and insulin secretion: their role in health and disease. Diabetologia; 42(8):903-19.

Baughman, J.M., Perocchi, F., Girgis, H.S., Plovanich, M., Belcher-Timme, C.A., Sancak, Y., Bao, X.R., Strittmatter, L., Goldberger, O., Bogorad, R.L., et al. (2011). Integrative genomics identifies MCU as an essential component of the mitochondrial calcium uniporter. Nature 476, 341-345.

Blinks, J.R. (1978). Applications of calcium-sensitive photoproteins in experimental biology. Photochem Photobiol *27*, 423-432.

Brini, M. (2008). Calcium-sensitive photoproteins. Methods 46, 160-166

Cahalan MD, Chandy KG (2009). The functional network of ion channels in T lymphocytes. Immunol Rev 231:59-87.

Cheng Y, Gu XQ, Bednarczyk P, Wiedemann FR, Haddad GG, Siemen D (2008). Hypoxia increases activity of the BK-channel in the inner mitochondrial membrane and reduces activity of the permeability transition pore. Cell Physiol Biochem 22:127-136.

Cobbold, P.H., and Bourne, P.K. (1984). Aequorin measurements of free calcium in single heart cells. Nature 312, 444-446.

Cohen MV, Baines CP, Downey JM. (2000). Ischemic preconditioning: from adenosine receptor to K(ATP) channel. Annu Rev Physiol.; 62: 79-109.

Davis N.W., Standen N.B., Stanfield P.R. (1991). ATP-dependent potassium channels of muscle cells: their properties, regulation, and possible functions. J. Bioenerg. Biomembranes 23, 509-535.

Dean, M. and Allikmets, R. 1995. Evolution of ATP-binding cassette transporter genes. Curr. Opin. Genet. Dev. 5: 779–785.

De Marchi U, Checchetto V, Zanetti M, Teardo E., Soccio M, Formentin E, Giacometti GM, Pastore D, Zoratti M, Szabò I (2010). ATP-sensitive cation-channel in wheat (Triticum durum Desf.): identification and characterization of a plant mitochondrial channel by patch-clamp. Cell Physiol Biochem 26(6):975-982, Epub 2011 Jan 4.

De Stefani, D., Raffaello, A., Teardo, E., Szabo, I., and Rizzuto, R. (2011). A forty-kilodalton protein of the inner membrane is the mitochondrial calcium uniporter. Nature 476, 336-340.

Diwan J.J., Haley T., Sanadi D.R. (1988). Reconstitution of transmembrane K+ transport with a 53 kilodalton mitochondrial protein. Biochem. Biophys. Res. Commun. 153, 224-230.

Duarte, J.M., Schuck, P.F., Wenk, G.L., and Ferreira, G.C. (2014). Metabolic disturbances in diseases with neurological involvement. Aging Dis 5, 238-255.

Duchen, M.R. (2004). Roles of mitochondria in health and disease. Diabetes 53 Suppl 1, S96-102.

Edwards G, Weston AH. (1993). The pharmacology of atp-sensitive potassium channels. Annu. Rv. Pharmacol. Toxicol. 33:597-637.

Fieni F., Parkar A., Misgeld T., Kerschensteiner M., Lichtman JW, Pasinelli P., Trotti D. (2010). Voltage-dependent inwardly rectifying potassium conductance in the outer membrane of neuronal mitochondria. J Biol Chem 285:27411-27417.

Forbes R.A., Steenbergen C., Murphy E. (2001) Diazoxide-induced cardioprotection requires signaling through a redox-sensitive mechanism. Circ Res.; 88: 802-9.

Garlid K.D., Halestrap A.P. (2012). The mitochondrial K(ATP) channel—fact or fiction? J. Mol. Cell. Cardiol. 52(3):578-83.

Garlid K.D., Dos Santhos P., Xie Z., Paucek P. (2003). Mitochondrial potassium transport: the role of the mitochondrial ATP-sensitive K+ channel in cardiac function and cardioprotection. Biochimic. Biophys. Acta 1606.

Garlid K.D, Paucek P., Yarov-Yarovoy V., Murray H.N., Darbenzio R.B, D'Alonzo A.J, Lodge N.J., Smith M.A, Grover G.J. (1997). Cardioprotective effect of diazoxide and its interaction with mitochondrial ATP-sensitive K+ channels. Possible mechanism of cardioprotection. Circ. Res. 81, 1072-1082.

Gaude, E., and Frezza, C. (2014). Defects in mitochondrial metabolism and cancer. Cancer Metab 2, 10.

Grover G.J, Garlid K.D. (2000). ATP-sensitive potassium channels: a review of their cardioprotective pharmacology. J Mol Cell Cardiol.; 32: 677-95.

Grover J.D, McCullough J.R., Henry D.E., Conder M.L., Sleph P.G. (1989). Anti-ischemic effects of the potassium channel activators pinacidil and cromakalim and the reversal of these effects with the potassium channel blocker glyburide. J. Pharmacol. Exp. Ther. 251, 98-104.

Halestrap A.P. (1989). The regulation of the matrix volume of mammalian mitochondria in vivo and in vitro and its role in the control of mitochondrial metabolism. Biochim Biophys Acta.; 973: 355-82.

Hartl, F.U., Pfanner, N., Nicholson, D.W., and Neupert, W. (1989). Mitochondrial protein import. Biochim Biophys Acta 988, 1-45.

Hayashi T., Rizzuto R., Hajnoczky G., Su TP. (2009). MAM: more than just a housekeeper. Trends Cell Biol 19:81-88.

Heinen A, Camara AK, Aldakkak M, Rhodes SS, Riess ML, Stowe DF (2007). Mitochondrial Ca^{2+}-induced K^{+} influx increases respiration and enhances ROS production while maintaining membrane potential. Am J Physiol Cell Physiol 292:C148-C156.

Higgins, C.F. 1992. ABC transporters: From micro-organisms to man. Annu. Rev. Cell. Biol. 8: 67–113.

Hogue DL, Liu L, Ling V (1999) Identification and characterization of a mammalian mitochondrial ATP-binding cassette membrane protein. J Mol Biol 285:379–389.

Holmuhamedov E.L., Wang L., Terzic A. (1999). ATP-sensitive K+ channel openers prevent Ca2+ overload in rat cardiac mitochondria. J Physiol (Lond).; 519 (Pt2): 347-60.

Ichikawa Y., Bayeva M., Ghanefar M., Potini V., Sun L., Mutharasan R.K., Wu R.,Khechaduri A., Jairaj Naik T., and Ardehali H. (2012). Disruption of ATP-binding cassette B8 in mice leads to cardiomyopathy through a decrease in mitochondrial iron export. PNAS 109(11): 4152-4157.

Inoue, I., Nagase, H., Kishi, K., and Higuti, T. (1991). ATP-sensitive K+ channel in the mitochondrial inner membrane. Nature 352, 244-247.

Kaul S., Anantharam V., Kanthasamy A., Kanthasamy AG. (2005). Wild-type alpha-synuclein interacts with pro-apoptotic proteins PKCdelta and BAD to protect dopaminergic neuronal cells against MPP+ induced apoptotic cell death. Brain Res Mol Brain Res 139:137-152.

Kloner R.A, Bolli R., Marban E., Reinlib L., Braunwald E. (1986) Medical and cellular implications of stunning hibernation, and preconditioning: an NHLBI workshop. Circulation.; 97: 1848-67.

Kosztka L., Rusznàk Z., Nagy D., Nagy Z., Fodor J., Szucs G., Telek A., Gönczi M., Ruzsnavsky O., Szentandràssy N., Csernoch L. (2011). Inhibition of TASK-3 (KCNK9) channel biosynthesis changes cell morphology and decreases both DNA content and mitochondrial function of melanoma cells maintained in cell culture. Melanoma Res 21:308-322.

Mannella, C.A. (2006). Structure and dynamics of the mitochondrial inner membrane cristae. Biochim Biophys Acta 1763, 542-548.

Mironova G.D, Fedotcheva N.I., Makarov P.R., Pronevich L.A., Mironov G.P. (1981). Protein from beef heart mitochondria inducing the potassium channel conductivity of bilayer lipid membrane. Biophysik (USSR) 26, 458-465.

Mitchell, P. (1966). Chemiosmotic coupling in oxidative and photosynthetic phosphorylation. Biol Rev Camb Philos Soc 41, 445-502.

Murata M, Akao M, O' Rourke B, Marban E. (2001). Mitochondrial ATP-sensitive potassium channels attenuate matrix Ca2+ overload during simulated ischemia and reperfusion: possible mechanism of cardioprotection. Circ Res.; 89: 891-8.

Murry C.E., Jennings R.B., Reimer K.A. (1986). Preconditioning with ischemia: a delay of lethal cell injury in ischemic myocardium. Circulation.; 74: 1124-36.

Nichols C.G., Shyng S.L., Nestorowicz A., Glaser B., Clement J.P., Gonzalez G., Aguilar-Bryan L., Permutt M.A., Bryan J. (1996). Adenosine diphosphate as an intracellular regulator of insulin secretion. Science 272, 1785-1787.

Noma A. (1983) ATP-regulated K+ channels in cardiac muscle. Nature. 305: 147-8.

O'Rourke B. (2000) Myocardical K(ATP) channels in preconditioning. Circ Res.; 87: 845-855.

O'Rourke, B. (2004). Evidence for mitochondrial K+ channels and their role in cardioprotection. Circ. Res. 94, 420-432.

Ozcan C, Bienengraeber M, Dzeja PP, Terzic A. (2002). Potassium channel openers protect cardiac mitochondria by attenuating oxidant stress at reoxygenation. Am j Physiol Heart Circ Physiol.; 282: H531-9.

Pain T, Yang XM, Critz SD, Yue Y, Nakano A, Liu GS, Heusch G, Cohen MV, Downey JM (2000). Opening of mitochondrial K(ATP) channels triggers the preconditioned state by generating free radicals. Circ Res.; 87: 460-6.

Patel A.J., Lazdunski M. (2004). The 2P-domain K+ channels: role in apoptosis and tumorigenesis. Pflugers Arch 448: 261-273.

Patron, M., Raffaello A., Granatiero V., Tosatto A., Merli G., De Stefani D., Wright L., Pallafacchina G., Terrin A., Mammucari C., Rizzuto R. (2013). The mitochondrial calcium uniporter (MCU): molecular identity and physiological roles. J. Biol Chem 288(15): 10750-8.

Perocchi, F., Gohil, V.M., Girgis, H.S., Bao, X.R., McCombs, J.E., Palmer, A.E., and Mootha, V.K. (2010). MICU1 encodes a mitochondrial EF hand protein required for Ca(2+) uptake. Nature 467, 291-296.

Raffaello, A., De Stefani, D., Sabbadin, D., Teardo, E., Merli, G., Picard, A., Checchetto, V., Moro, S., Szabo, I., and Rizzuto, R. (2013). The mitochondrial calcium uniporter is a multimer that can include a dominant-negative pore-forming subunit. EMBO J 32, 2362-2376.

Rizzuto, R., Pinton, P., Carrington, W., Fay, F.S., Fogarty, K.E., Lifshitz, L.M., Tuft, R.A., and Pozzan, T. (1998). Close contacts with the endoplasmic reticulum as determinants of mitochondrial Ca^{2+} responses. Science 280, 1763-1766.

Rizzuto, R., Simpson, A.W., Brini, M., and Pozzan, T. (1992). Rapid changes of mitochondrial Ca^{2+} revealed by specifically targeted recombinant aequorin. Nature 358, 325-327.

Roszik J., Szöllo''si J., Vereb G. (2008). AccPbFRET: an ImageJ plugin for semi-automatic, fully corrected analysis of acceptor photobleaching FRET images. BMC Bioinformatics 9:346, 1471-2105.

Rozen, S., and Skaletsky, H. (2000). Primer3 on the WWW for general users and for biologist programmers. Methods Mol Biol 132, 365-386.

Rusznàk, Z., Bakondi, G., Kosztka, L., Pocsai, K., Diens, B., Fodor, J., Telek, A., Gömczi, M., Szücs, G., and Csernoch, L. (2008). Mitochondrial expression of the two pore domain TASK-3 channels in malignantly transformed and non-malignant human cells. Virchows Arch. 452, 415-426.

Sassi N., De Marchi U., Fioretti B., Biasutto L., Gulbins E., Francolini F., Sbazò I., Zoratti M. (2010). An investigation of the occurrence and properties of the mitochondrial intermediate-conductance Ca2+-activated K+ channel mtKCa3.1. Biochim Biophys Acta Bioenergetics 1797: 260-1267.

Sato T, Sasaki N, Seharaseyon J, O'Rourke B, Marban E. (2000). Selective pharmacological agents implicate mitochondrial but not sarcolemma KATP channels in ischemic cardioprotection. Circulation. 101(20):2418-23.

Shimomura, O. (1986). Isolation and properties of various molecular forms of aequorin. Biochem J 234, 271-277.

Siemen, D., Loupatatzis, C., Borecky, J., Gulbins, E., and Lang, F. (1999). Ca^{2+}-activated K channel of the BK-type in the inner mitochondrial membrane of a human glioma cell line. Biochem. Biophys. Res. Commun. 257, 549-554.

Szabò, I., Zoratti M. (2014). Mitochondrial channels: ion fluxes and more. Physiol Rev 94: 519-608.

Szabò, I., Soddeman, M., Leanza L., Zoratti, M., Gulbins E. (2011). Single point mutations of a lysine residue change function of Bax and Bcl-XL expressed in Bax- and Bak-less mouse embryonic fibroblasts: novel insights into the molecular mechanisms of Bax- induced apoptosis. Cell Death Differ. 18, 427-438.

Szabò, I., Bock, J., Jekle, A., Soddemann, M., Adams, C., Lang, F., Zoratti, M., and Gulbins, E. (2005). A novel potassium channel in lymphocyte mitochondria. J. Biol. Chem. 280, 12790-12798.

Szewczyk, A. and Marban, E. (1999). Mitochondria: a new target for K channel openers? Trends Pharmacol. Sci. 20, 157-161.

Skalska J, Bednarczyk P, Piwon'ska M, Kulawiak B, Wilczynski G, Dolowy K, Kudin AP, Kunz WS, Szewczyk A. (2009). Calcium ions regulate K+ uptake into brain mitochondria: the evidence for a novel potassium channel. Int J Mol Sci 10:1104-1120.

Skalska J, Bednarczyk P, Piwon'ska M, Kulawiak B, Wilczynski G, Dolowy K, Kudin AP, Kunz WS, Szewczyk A. (2008). A novel potassium channel in skeletal muscle mitochondria. Biochim Biophys Acta 1777: 651-659.

Szewczyk, A., Jarmuszkiewicz, W., S. Kunz, W. (2009). Mitochondrial Potassium Channels. IUBMB Life, 61(2): 134-143.

Teardo, E. et al. (2010). Characterization of a plant glutamate receptor activity. Cell Physiol. Biochem. 26, 253-262.

van der Krogt, G. N., J. Ogink, et al. (2008). "A comparison of donor-acceptor pairs for genetically encoded FRET sensors: application to the Epac cAMP sensor as an example." PLoS One 3(4): e1916.

Vanden Hoek TL, Becker LB, Shao Z, Li C, Schumacker PT. (1998). Reactive oxygen species released from mitochondria during brief hypoxia induce preconditioning in cardiomyocytes. J Biol Chem.; 273: 18092-8.

Wallace D.C (2005). The mitochondrial genome in human adaptive radiation and disease: on the road to therapeutics and performance enhancement. Gene 354;169-180.